PHYSICAL REVIEW C VOLUME 27, NUMBER 4 APRIL 1983

Pion single and double charge exchange in the resonance region: Dynamical corrections

Mikkel B. Johnson
Los Alamos National Laboratory, Los Alamos, New Mexico 87545

E. R. Siciliano*
Nuclear Physics Laboratory, University of Colorado, Boulder, Colorado 80309
and Los Alamos National Laboratory, Los Alamos, New Mexico 87545
(Received 8 November 1982)

We consider pion-nucleus elastic scattering and single- and double-charge-exchange scattering to isobaric analog states near the (3,3) resonance within an isospin invariant framework. We extend previous theories by introducing terms into the optical potential U that are quadratic in density and consistent with isospin invariance of the strong interaction. We study the sensitivity of single and double charge exchange angular distributions to parameters of the second-order potential both numerically, by integrating the Klein-Gordon equation, and analytically, by using semiclassical approximations that explicate the dependence of the exact numerical results to the parameters of U. The magnitude and shape of double charge exchange angular distributions are more sensitive to the isotensor term in U than has been hitherto appreciated. An examination of recent experimental data shows that puzzles in the shape of the $^{18}O(\pi^+,\pi^-)^{18}Ne$ angular distribution at 164 MeV and in the A dependence of the forward double charge exchange scattering on ^{18}O, ^{26}Mg, ^{42}Ca, and ^{48}Ca at the same energy may be resolved by adding an isotensor term in U.

[NUCLEAR REACTIONS Scattering theory for elastic, single-, and double-charge-exchange scattering to IAS in the region of the $P33$ resonance. Second-order effects on charge-exchange calculations of $\sigma(A,\theta)$.]

I. INTRODUCTION

Pion elastic scattering and single- (SCX) and double-charge-exchange (DCX) scattering to the isobar analog states are related in a simple way by the isospin symmetry of the underlying strong interactions. The meson factories are now beginning to acquire complete sets of data of this type for a variety of nuclear targets. In order to interpret these data, an optical potential theory which deals correctly with isospin at a fundamental level is needed. Although previous work[1] on charge exchange has incorporated many of the necessary elements of the basic theory, it has been tied closely to theoretical models which deal only partially with the pion-nucleus dynamics. What is needed, rather, is a framework which incorporates the well-known theoretical elements of pion-nucleus scattering, and includes adjustable parameters to fit the remaining discrepancies in the data. With a sufficiently careful, theoretically motivated parametrization of the optical potential U, the values for the parameters fitted to the data will carry significant and presumably interpretable information about the unknown dynamics of the pion-nucleus interaction and the structure of the nuclear target.

In a previous paper[2] (hereafter referred to as I), analytic approximations were developed for angular distributions of SCX and DCX scattering to isobaric analog states near the (3,3) resonance. A special case was examined in detail, namely that in which U includes only terms of lowest order in the nuclear density. In this model the analytic results explicated the dependence of the angular distribution on the geometrical properties of the nucleus—the dependence on a radius $\bar{R}$, diffuseness of neutron and proton distributions, and the relative nucleon density at $\bar{R}$. The simple theory reasonably described the *relative* A and $N-Z$ dependence of the empirical zero degree SCX scattering[2,3] throughout the periodic table and also that for DCX at 292 MeV.[4] However, the theory failed to reproduce the empirical values of the absolute magnitude of the SCX and DCX angular distributions at 0°. It also failed to reproduce the shape of the known DCX angular distribution at 164 MeV.[2] The shortcomings found in

the analytical theory are also found in computer solutions of the Klein-Gordon equation with lowest-order potentials.

The failure of the theory lies presumably in the fact that the reaction theory implicit in the lowest-order optical potential is too naive. The second-order optical potential is discussed in detail in a previous paper,[5] where its dependence on the nuclear isospin and on the density distributions is derived. The goal of the present paper is to extend existent theories of U for scattering near the (3,3) resonance by including the second-order potential of Ref. 5 and to obtain a physical understanding of the variety of physics embodied in the theory by extending the analytic results of I.

In Sec. II we propose an isospin invariant theory for the first- plus second-order optical model potential. Analytic expressions for SCX and DCX cross sections are derived in Sec. III. In Sec. IV we use the analytic theory in conjunction with the numerical solution of the Klein-Gordon equation to explore the systematics of charge exchange scattering at resonance in our theory, and in Sec. V we discuss experimental implications of the theory.

II. BASIC THEORY

In this paper we assume that the optical potential has the form

$$U=\vec{\nabla}\cdot[\xi(r)+\Delta\xi(r)]\vec{\nabla}-k^2[\bar{\xi}(r)+\Delta\bar{\xi}(r)] -\tfrac{1}{2}(p_1-1)\nabla^2\xi(r)-\tfrac{1}{2}(p_2-1)\nabla^2\Delta\xi(r)\,, \quad (2.1a)$$

where $\bar{\xi}(r)$ and $\xi(r)$ are, respectively, the S- and P-wave contributions to the lowest-order optical potential; $\Delta\bar{\xi}(r)$ and $\Delta\xi(r)$ refer, similarly, to the higher-order contributions. The form chosen is basically the same as originally proposed by Kisslinger[6] and subsequently modified as in Refs. 7–12. The quantities p_1 and p_2 are kinematical factors that result from a frame transformation, which we take as

$$p_1=\frac{1+\epsilon}{1+\epsilon/A}\,, \quad (2.1b)$$

$$p_2=\frac{1+\epsilon/2}{1+\epsilon/A}\,, \quad (2.1c)$$

where

$$\epsilon=\omega/M\,, \quad (2.1d)$$

ω is the pion total energy in the pion-nucleus center of mass system, and M is the nucleon mass ($\hbar=c=1$). This form for U was used recently in an extensive theoretical study of pion-nucleus elastic and inelastic scattering from low energy[11] (50 MeV) through the region of the (3,3) resonance.[12] The focus of attention in this work was the role of higher-order terms in the optical potential, and it was found that the optical potential given in Eqs. (2.1) adequately described elastic scattering provided such terms were included. However, the isospin dependence in these works was treated too crudely for the purpose of describing charge exchange.

Because our main interest is SCX and DCX to isobaric analog states, we choose to describe the scattering by an optical potential that couples explicitly the ground state, single- and double-analog states. To the extent that intermediate excitations to nonanalog states are important and that higher-order dynamical effects contribute, U must include terms of second order (and higher) in density. The most general dependence of U on the pion isospin $\vec{\phi}$ that accomplishes this is easily obtained, assuming that the underlying interactions are isospin invariant. There is no strong empirical evidence that isospin invariance is significantly violated in strong interactions, and thus we write for both S and P waves

$$\xi=\xi_0+\xi_1(\vec{\phi}\cdot\vec{\mathrm{T}}) \quad (2.2a)$$

and

$$\Delta\xi=\Delta\xi_0+\Delta\xi_1(\vec{\phi}\cdot\vec{\mathrm{T}})+\Delta\xi_2(\vec{\phi}\cdot\vec{\mathrm{T}})^2\,, \quad (2.2b)$$

where $\vec{\mathrm{T}}$ the nuclear isospin operator. Isospin invariance requires that the terms linear in density have the following form:

$$\xi_0=\lambda_0^{(1)}\rho(r),\quad \xi_1=\frac{1}{2T}\lambda_1^{(1)}\Delta\rho(r)\,, \quad (2.3)$$

where $\lambda_0^{(1)}$ and $\lambda_1^{(1)}$ are complex parameters, T is the isospin of the target nucleus, and ρ ($\Delta\rho$) is the sum (difference) of neutron and proton densities. The parameters $\lambda^{(1)}$ are related to the free pion-nucleon phase shifts. The relationship is expressed in Refs. 11 and 12 in terms of parameters b_0, b_1, c_0, and c_1, which are in turn related to the $\lambda^{(1)}$ of our paper by

$$\bar{\lambda}_0^{(1)}=4\pi p_1 b_0/k^2\,, \quad (2.4a)$$

$$\bar{\lambda}_1^{(1)}=8\pi p_1 b_1/k^2\,, \quad (2.4b)$$

$$\lambda_0^{(1)}=\frac{4\pi}{p_1}c_0\,, \quad (2.4c)$$

$$\lambda_1^{(1)}=\frac{8\pi}{p_1}c_1\,. \quad (2.4d)$$

In Refs. 8–12 the pion-nucleon phase shifts are evaluated at a center-of-mass energy equal to the center-of-mass pion-nucleus energy. This is a bad approximation in the resonance region where the pion-nucleon amplitude varies rapidly as a function of energy. Corrections arising from the recoil of the pion-nucleon system can be described approximately as: (1) a shift in the energy at which the pion-

nucleon amplitude is evaluated in the medium[13] and (2) an increase in the width of the (3,3) resonance.[14] We fix the amount of the energy shift by including a parameter ΔE which moves the energy at which the pion-nucleon phase shifts are evaluated. Theory[13] and phenomenological analysis[15,16] suggest that $\Delta E \simeq -20$ to -30 MeV, i.e., the pion-nucleon amplitude is to be evaluated at an energy *less than* the incident energy by this amount. As there are no corresponding quantitative theoretical or phenomenological estimates for the Fermi broadening, we have not made any adjustment of the lowest-order parameters for this effect. We believe that this omission will not affect the qualitative conclusions of this work.

As for the higher-order terms, we have derived in a previous paper[5] the dependence of $\Delta\xi$ on T, ρ, and $\Delta\rho$. For zero-ranged pion-nucleon form factors the S- and P-wave pieces of $\Delta\xi$ have the same form,

$$\Delta\xi_0=\lambda_0^{(2)}\frac{\rho^2}{\rho_0}+\lambda_3^{(2)}\frac{\Delta\rho^2}{\rho_0}-\frac{1}{2T-1}\lambda_2^{(2)}\frac{\Delta\rho^2}{\rho_0}\ , \tag{2.5a}$$

$$\Delta\xi_1=\frac{\lambda_1^{(2)}}{2T}\frac{\rho\Delta\rho}{\rho_0}+\frac{\lambda_2^{(2)}}{2T(2T-1)}\frac{\Delta\rho^2}{\rho_0}\ , \tag{2.5b}$$

$$\Delta\xi_2=\frac{\lambda_2^{(2)}}{T(2T-1)}\frac{\Delta\rho^2}{\rho_0}+\frac{\lambda_4^{(2)}}{T^2}\frac{\Delta\rho^2}{\rho_0}\ , \tag{2.5c}$$

where $\rho_0=0.16$ fm^{-3} is the central density of heavy nuclei and is introduced so that the first- and second-order parameters $\lambda^{(1)}$ and $\lambda^{(2)}$ have the same units. As shown in Ref. 5, the r dependence of $\lambda^{(2)}$ is weak, and we therefore assume that all the r dependence occurs through the factors of ρ and $\Delta\rho$. The constraints imposed by isospin invariance have resulted in the quadratic terms $\Delta\xi$ being described by five complex parameters, four of which are theoretically uncertain. As a phenomenological form for the second-order optical potential, the important characteristics[5] of Eq. (2.5) are the following: (1) one set of parameters characterizes elastic, SCX, and DCX scattering from a given target at a given energy; (2) nontrivial models of the pion-nucleus interaction exist for which the parameter set may be evaluated; (3) the parameters are independent of $N-Z$ and only weakly dependent on A of the target nucleus; and (4) the parameters can be expected to be strongly energy dependent.

The Coulomb interaction is not included in our above description of charge exchange. The arguments for omitting it are the following. In Refs. 17–19 it was shown that the net effect of the Coulomb interaction is close to zero for both SCX and DCX in the absence of Coulomb mixing in the nuclear wave function. The corrections for Coulomb mixing have been studied in Ref. 20. It is argued there that at least for the SCX reaction, $\Delta\rho$ should be reinterpreted as the *valence* neutron density. Thus, to a first approximation the effects of the Coulomb interaction may be handled in our isospin invariant framework. The corrections arising from the approximate handling of Coulomb effects may presumably be included by adding *small* isospin breaking terms to U, whose effect can be evaluated perturbatively in practice.

To obtain the appropriate pion-nucleus scattering amplitudes that result from U given in Eqs. (2.1)–(2.5), it is useful to project U onto channels of total isospin $\vec{\tau}=\vec{\phi}+\vec{T}$, where the optical potential becomes diagonal. In this case we find

$$U_\tau=\vec{\nabla}\cdot[\xi_\tau(r)+\Delta\xi_\tau(r)]\vec{\nabla}-k^2\xi_\tau(r)-k^2\Delta\xi_\tau(r)$$
$$-\tfrac{1}{2}(p-1)\nabla^2[\xi_\tau(r)+\Delta\xi_\tau(r)]\ , \tag{2.6a}$$

where we have introduced a compact notation for the factors of p_1 and p_2 of Eq. (2.1): The quantity p is p_1 whenever it multiplies $\lambda^{(1)}$ and p_2 whenever it multiplies $\lambda^{(2)}$. The projection of ξ is easily accomplished [see Eq. (5) of I] and the results for ξ_τ obtained from Eqs. (2.2), (2.3), and (2.5) are

$$\xi_\tau(r)=\lambda_0^{(1)}\rho(r)+\gamma^{(1)}(\tau)\lambda_1^{(1)}\Delta\rho(r)\ , \tag{2.6b}$$

$$\Delta\xi_\tau(r)=\lambda_0^{(2)}\frac{\rho^2}{\rho_0}+\gamma^{(1)}(\tau)\lambda_1^{(2)}\frac{\rho\Delta\rho}{\rho_0}+\gamma^{(2)}(\tau)\lambda_2^{(2)}\frac{\Delta\rho^2}{\rho_0}+[\gamma^{(4)}(\tau)\lambda_4^{(2)}+\lambda_3^{(2)}]\frac{\Delta\rho^2}{\rho_0}\ , \tag{2.6c}$$

where

$$\gamma^{(4)}(\tau)=\frac{1}{T}[1-\gamma^{(1)}(\tau)+(2T-1)\gamma^{(2)}(\tau)]\ , \tag{2.6d}$$

and where $\gamma^{(1)}(\tau)$ and $\gamma^{(2)}(\tau)$ are given in Table I.

We have written a computer program PIESDEX, using a modified version of the program PIRK,[21] to enable us to find the exact numerical solution of the Klein-Gordon equation. Our procedure in PIESDEX is to first obtain pion-nucleus scattering amplitudes on total isospin channels that result from U_τ given by Eqs. (2.6). Then we construct the elastic, SCX, and DCX amplitudes by taking the appropriate linear combinations[2] of the total isospin amplitudes. In Sec. IV we will study these solutions in detail.

TABLE I. Values for $\gamma^{(i)}(\tau)$.

τ	$T-1$	T	$T+1$
$\gamma^{(1)}(\tau)$	$-\left\lfloor\frac{T+1}{2T}\right\rfloor$	$-\frac{1}{2T}$	$\frac{1}{2}$
$\gamma^{(2)}(\tau)$	$\frac{2T^2+T+1}{2T(2T-1)}$	$-\frac{1}{2T}$	$\frac{1}{2}$

III. EIKONAL THEORY

In the region of the (3,3) resonance, strong pion absorption causes pion-nucleus scattering to be diffractive. This diffractive behavior lends itself to a semiclassical treatment of the scattering, and such an approach can yield simple analytic formulas that are qualitatively successful, especially for elastic scattering. Such formulas have been very useful in understanding more complicated calculations, as well as systematics of data. We are therefore motivated to find analogous analytic results for SCX and DCX reactions for the theory which includes terms quadratic in density.

In this section we develop analytic formulas for SCX and DCX by extending the techniques used in Refs. 2, 22, and 23. Our objective in obtaining these results is to explicate their dependence on the $\lambda^{(2)}$ parameters of Eq. (2.5). The manipulations involved are somewhat lengthy, so for the case of presentation we have relegated most of the details to the appendices. The present section is basically a sketch of our procedures, with a display in Eqs. (3.17) and (3.18) of our analytic formulas for SCX and DCX. The more casual reader may wish to simply observe Eqs. (3.17) and (3.18) and proceed ahead to the next section. The details in the appendices are necessary, however, to trace the coefficients characterizing the scattering amplitude back to the parameters in U.

In order to apply the analytic eikonal theory of Refs. 22 and 23, U must be local. The U in Eq. (2.6) is nonlocal, and the transformation discussed in Appendix A must be performed. Once the local potential is obtained, the eikonal phase function $\tilde{\chi}(b)$ may be calculated from

$$\tilde{\chi}_\tau(b)=\frac{1}{2k}\int_{-\infty}^{\infty}\left\{U_\tau(r)+\frac{1}{4k^2}\left[U_\tau^2(b)+\frac{b^2}{r^2}\frac{d}{dr}U_\tau^2(b)\right]\right\}dz\ . \tag{3.1}$$

The terms in the square brackets in Eq. (3.1) are the lowest-order corrections in k^{-2} derived by Wallace.[24] These terms are needed to compare the eikonal theory to the solution of the Klein-Gordon equation. We consider the lowest-order Wallace corrections because they contain terms of order ρ^2 and are therefore of the same order in density as the second-order terms in U. We ignore the remaining Wallace corrections because they are higher order in density and k^{-2} and are therefore presumably less important.

In Ref. 22 an approximation to $\chi_\tau(b)$ was derived that worked well when the impact parameter b was comparable to the nuclear radius, and when $U(r)$ was linear in density. In Appendix A we derive a result for $\tilde{\chi}(b)$ valid when U contains second-order terms. The result is

$$\begin{aligned}\frac{2k\tilde{\chi}_\tau(b)}{k^2(2\pi a_\rho b)^{1/2}}=&\Lambda_0^{(1)}\rho+\Lambda_1^{(1)}\Delta\rho\gamma^{(1)}(\tau)\\&+\tilde{\Lambda}_0^{(2)}\frac{\rho^2}{\rho_0}+\tilde{\Lambda}_1^{(2)}\frac{\rho\Delta\rho}{\rho_0}\gamma^{(1)}(\tau)\\&+\tilde{\Lambda}_2^{(2)}\frac{\Delta\rho^2}{\rho_0}\gamma^{(2)}(\tau)+\tilde{\Lambda}_4^{(2)}\frac{\Delta\rho^2}{\rho_0}\gamma^{(4)}(\tau)\\&+\tilde{\Lambda}_5^{(2)}\frac{\Delta\rho^2}{\rho_0}[\gamma^{(1)}(\tau)]^2\ ,\end{aligned} \tag{3.2}$$

where in Appendix A the coefficients $\Lambda^{(1)}$ and $\tilde{\Lambda}^{(2)}$ are given explicitly in terms of the $\lambda^{(1)}$ and $\lambda^{(2)}$ parameters of Eq. (2.6), and

$$a_\rho=-\frac{2k^2\rho(b)+p_1\nabla^2\rho(b)}{2k^2\rho'(b)+p_1\nabla^2\rho'(b)}\ . \tag{3.3}$$

The amplitude for scattering in an uncoupled channel of total isospin τ is, according to the theory of Refs. 22 and 23,

$$\begin{aligned}F_\tau(\theta)\equiv&F(\theta,R_\tau,A_\tau)\\=&ikR_\tau^2\frac{J_1(qR_\tau)}{qR_\tau}+A_\tau R_\tau J_0(qR_\tau)\ ,\end{aligned} \tag{3.4a}$$

where

$$\begin{aligned}A_\tau=&ika_\tau[C+\ln(\ln 2)+\tfrac{1}{2}\ln(1+Y_\tau^2)]\\&+ka_\tau\tan^{-1}Y_\tau\ ,\end{aligned} \tag{3.4b}$$

with $C\simeq 0.5772$ being Euler's constant and the J's Bessel functions. The quantities R_τ, a_τ, and Y_τ are related directly to U through $\tilde{\chi}(b)$:

$$Y_\tau=\mathrm{Re}\tilde{\chi}_\tau(\bar{R})/\mathrm{Im}\tilde{\chi}_\tau(\bar{R})\ , \tag{3.4c}$$

$$a_\tau=-\mathrm{Im}\tilde{\chi}_\tau(\bar{R})/\mathrm{Im}\tilde{\chi}'_\tau(\bar{R})\ . \tag{3.4d}$$

The radius R_τ is determined from the equation

$$\mathrm{Im}\tilde{\chi}(R_\tau)=\ln 2 \ , \tag{3.4e}$$

and $\bar{R}$ is an appropriate average of R_τ, defined below. In Ref. 23 corrections to Eq. (3.4a) were obtained, the most important of which is an overall multiplicative factor $\Gamma(1-a_\tau q)$ (the so-called Inopin factor) which gives F the correct average rate of falloff in angle. Here Γ is the gamma (factorial) function.

In I, expressions for the charge-exchange amplitudes valid through second order in density were obtained. The results of that paper for the SCX and DCX amplitudes are

$$F^{(0+)}(\theta)=\frac{1}{\sqrt{T}}\frac{1}{2T+1}\frac{1}{T+1}\left[S^{(0+)}\frac{\partial F}{\partial \bar{R}}(\theta,\bar{R})+P^{(0+)}\frac{\partial^2 F}{\partial \bar{R}^2}(\theta,\bar{R})\right] \tag{3.5a}$$

and

$$F^{(-+)}(\theta)=-\left[\frac{2T-1}{T}\right]^{1/2}\frac{1}{T+1}\frac{1}{2T+1}\left[S^{(-+)}\frac{\partial F}{\partial \bar{R}}(\theta,\bar{R})+P^{(-+)}\frac{\partial^2 F}{\partial \bar{R}^2}(\theta,\bar{R})\right] , \tag{3.5b}$$

where the S and P coefficients are expressed as differences of the strong absorption radii R_τ determined by Eq. (3.4e),

$$S^{(0+)}=(2T^2-1)(R_T-R_{T-1})+T(R_{T+1}-R_T)+T(R_{T+1}-R_{T-1}) , \tag{3.6a}$$

$$P^{(0+)}=T(R_{T+1}-R_{T-1})(R_{T+1}-R_T) , \tag{3.6b}$$

$$S^{(-+)}=(T+1)(R_T-R_{T-1})-T(R_{T+1}-R_T) , \tag{3.6c}$$

$$P^{(-+)}=-\tfrac{1}{2}(2T+1)(R_{T+1}-R_T)(R_T-R_{T-1}) . \tag{3.6d}$$

Here $F(\theta,\bar{R})$ is the elastic scattering amplitude in the eikonal theory. Equations (3.5) and (3.6) were obtained in I from Eq. (3.4e), neglecting the dependence of A_τ on the quantum number τ; i.e., A_τ and Y_τ in Eq. (3.4b) were replaced by average values, $\langle a_\tau\rangle$ and $\langle Y_\tau\rangle$. In this case we found

$$\frac{\partial F}{\partial \bar{R}}=ik\bar{R}J_0(q\bar{R})+A[J_0(q\bar{R})-q\bar{R}J_1(q\bar{R})] , \tag{3.7a}$$

$$\frac{\partial^2 F}{\partial \bar{R}^2}=ik[J_0(q\bar{T})-q\bar{R}J_1(q\bar{R})]-Aq[J_1(q\bar{R})+q\bar{R}J_0(q\bar{R})] , \tag{3.7b}$$

where

$$\bar{R}=(R_T+R_{T-1})/2$$

for SCX,

$$\bar{R}=(R_{T+1}+R_{T-1})/2$$

for DCX, and

$$A=ik\langle a_\tau\rangle[C+\ln(\ln 2)+\tfrac{1}{2}\ln(1+\langle Y_\tau\rangle^2)]+k\langle a_\tau\rangle\tan^{-1}\langle Y_\tau\rangle . \tag{3.7c}$$

The Wallace corrections to $\tilde{\chi}$ are expressed in Eqs. (A9) and (A10) in terms of the quantity μ_i of Eq. (A10b). The μ_i are large even for a medium-heavy nucleus because the ratio $\bar{R}/a_\rho$ is a large number. At resonance, where the pion-nucleon scattering amplitude is purely imaginary, the Wallace correction to $\tilde{\chi}$ is purely real, enhancing the contribution of A_τ in Eq. (3.4b). It is therefore necessary to add correction terms to the results of I arising from the dependence of $F_\tau(\theta)$ on A_τ. This results in modifications to the $F^{(0+)}$ and $F^{(-+)}$ of I, as follows:

$$F^{(0+)}(\theta)\to F^{(0+)}(\theta)+\Delta F^{(0+)}(\theta) , \tag{3.8a}$$

$$F^{(-+)}(\theta)\to F^{(-+)}(\theta)+\Delta F^{(-+)}(\theta) . \tag{3.8b}$$

Expressions for ΔF are derived in Appendix B, and the main results for $\Delta F^{(0+)}$ are given in Eq. (B4) in terms of

$$\Delta S^{(0+)}=(2T^2-1)(A_T-A_{T-1})+T(2A_{T+1}-A_T-A_{T-1}) , \tag{3.9a}$$

$$\Delta P^{(0+)}=\tfrac{1}{2}(R_T-R_{T-1})\times[(2T^2-1)(A_T+A_{T-1}-2A_{T+1})-T(A_T-A_{T-1})] . \tag{3.9b}$$

The results for $\Delta F^{(-+)}$ are given in Eq. (B8) in terms of

$$\Delta S^{(-+)}=(T+1)(A_T-A_{T-1})-T(A_{T+1}-A_T) , \tag{3.10a}$$

$$\Delta P^{(-+)}=-\tfrac{1}{2}(R_{T+1}-R_{T-1})[(T+1)(A_T-A_{T-1}) +T(A_{T+1}-A_T)] . \tag{3.10b}$$

By combining the expression for $F^{(0+)}$ and $F^{(-+)}$ of I with the expressions for $\Delta F^{(0+)}$ and $\Delta F^{(-+)}$ of Appendix B, we find that the SCX and DCX amplitudes have the form, within our approximation scheme, of a linear combination of $J_0(q\bar{R})$ and

$$J_0(q\bar{R})-q\bar{R}J_1(q\bar{R}) .$$

The coefficients are worked out easily and the result is

$$F^{(0+)}(\theta)=\frac{1}{\sqrt{T}}\frac{1}{2T+1}\frac{\bar{R}}{T+1}\left\{J_0(q\bar{R})[ikS^{(0+)}+\Delta S^{(0+)}]+\frac{[J_0(q\bar{R})-q\bar{R}J_1(q\bar{R})]}{\bar{R}} \times[AS^{(0+)}+ikP^{(0+)}+\Delta P^{(0+)}]\right\}, \tag{3.11}$$

$$F^{(-+)}(\theta)=-\left[\frac{2T-1}{T}\right]^{1/2}\frac{1}{T+1}\frac{\bar{R}}{2T+1}\left\{J_0(q\bar{R})[ikS^{(-+)}+\Delta S^{(-+)}]+\frac{[J_0(q\bar{R})-q\bar{R}J_1(q\bar{R})]}{\bar{R}} \times[AS^{(-+)}+ikP^{(-+)}+\Delta P^{(-+)}]\right\} . \tag{3.12}$$

Through the coefficients S, P, ΔS, and ΔP, these expressions for the charge-exchange amplitudes depend upon the differences

$$\Delta R_{ij}\equiv R_i-R_j$$

and

$$\Delta A_{ij}=A_i-A_j .$$

Thus, within the eikonal theory the physics of SCX and DCX reduces to an understanding of these differences, which may be expressed in terms of quantities that appear in Eq. (3.2). The details are worked out in Appendix C where we obtain the following results. For ΔR we have

$$\Delta R_{ij}=a_\rho\left[\frac{\Delta\rho}{\rho}C_1\Gamma_{ij}^{(1)}+\left[\frac{\Delta\rho^2}{\rho\rho_0}\right]C_2\Gamma_{ij}^{(2)} -\frac{1}{2}\left[\frac{\Delta\rho}{\rho}\right]^2C_3\Gamma_{ij}^{(3)}+\frac{\Delta\rho^2}{\rho\rho_0}C_4\Gamma_{ij}^{(4)}\right] , \tag{3.13a}$$

where

$$\Gamma_{ij}^{(4)}=\frac{1}{T}[-\Gamma_{ij}^{(1)}+(2T-1)\Gamma_{ij}^{(2)}] , \tag{3.13b}$$

and where

$$C_1=\frac{W_1}{W_0}\frac{\mathrm{Im}\Lambda_0^{(1)}}{W_0} , \tag{3.13c}$$

$$C_2=\frac{\mathrm{Im}\tilde{\Lambda}_2^{(2)}}{W_0}\frac{\mathrm{Im}\Lambda_0^{(1)}}{W_0} , \tag{3.13d}$$

$$C_3=\left[\frac{W_1}{W_0}\right]^2\frac{\mathrm{Im}\Lambda_0^{(1)}}{W_0}+\phi\frac{W_1}{W_0}\frac{\rho}{\rho_0} -\frac{2\mathrm{Im}\Lambda_0^{(1)}}{W_0}\frac{\mathrm{Im}\tilde{\Lambda}_5^{(2)}}{W_0}\frac{\rho}{\rho_0} , \tag{3.13e}$$

$$C_4=\frac{\mathrm{Im}\tilde{\Lambda}_4^{(2)}}{W_0}\frac{\mathrm{Im}\Lambda_0^{(1)}}{W_0} , \tag{3.13f}$$

and

$$W_0=\mathrm{Im}\Lambda_0^{(1)}+\mathrm{Im}\tilde{\Lambda}_0^{(2)}\frac{\rho}{\rho_0} , \tag{3.13g}$$

$$W_1=\mathrm{Im}\Lambda_1^{(1)}+\mathrm{Im}\tilde{\Lambda}_1^{(2)}\frac{\rho}{\rho_0} , \tag{3.13h}$$

$$\phi=\frac{\mathrm{Im}\tilde{\Lambda}_1^{(2)}}{W_0}-\frac{\mathrm{Im}\tilde{\Lambda}_0^{(2)}}{W_0}\frac{W_1}{W_0} . \tag{3.13i}$$

For ΔA we have

$$\Delta A_{ij}=ka_\rho\left[\frac{\Delta\rho}{\rho}D_1\Gamma_{ij}^{(1)}+\left[\frac{\Delta\rho^2}{\rho\rho_0}\right]D_2\Gamma_{ij}^{(2)} +\left[\frac{\Delta\rho}{\rho}\right]^2D_3\Gamma_{ij}^{(3)}+\left[\frac{\Delta\rho^2}{\rho\rho_0}\right]D_4\Gamma_{ij}^{(4)}\right] , \tag{3.14a}$$

where

$$D_1=\frac{1}{1+y_0^2}\left[y_1-y_0\frac{W_1}{W_0}\right]\frac{\mathrm{Im}\Lambda_0^{(1)}}{W_0} , \tag{3.14b}$$

$$D_2=\left[\frac{\mathrm{Re}\tilde{\Lambda}_2^{(2)}-y_0\mathrm{Im}\tilde{\Lambda}_2^{(2)}}{W_0(1+y_0^2)}\right]\frac{\mathrm{Im}\Lambda_0^{(1)}}{W_0}\,, \tag{3.14c}$$

$$D_3=-\frac{\mathrm{Im}\Lambda_0^{(1)}}{W_0}\times\left\{\frac{W_1}{W_0}\left[y_1-y_0\frac{W_1}{W_0}\right]-\frac{\rho}{\rho_0}\left[\frac{\mathrm{Re}\tilde{\Lambda}_5^{(2)}-y_0\mathrm{Im}\tilde{\Lambda}_5^{(2)}}{W_0}\right]\right\}\frac{1}{1+y_0^2}\,, \tag{3.14d}$$

$$D_4=\left[\frac{\mathrm{Re}\tilde{\Lambda}_4^{(2)}-y_0\mathrm{Im}\tilde{\Lambda}_4^{(2)}}{W_0(1+y_0^2)}\right]\frac{\mathrm{Im}\Lambda_0^{(1)}}{W_0}\,, \tag{3.14e}$$

and

$$y_0=\frac{\mathrm{Re}\Lambda_0^{(1)}+\mathrm{Re}\tilde{\Lambda}_0^{(2)}\rho/\rho_0}{W_0}\,, \tag{3.14f}$$

$$y_1=\frac{\mathrm{Re}\Lambda_1^{(1)}+\mathrm{Re}\tilde{\Lambda}_1^{(2)}\rho/\rho_0}{W_0}\,. \tag{3.14g}$$

The $\Gamma_{ij}^{(l)}$ coefficients are given in Table II.

Since we are primarily interested in understanding the sensitivity of the cross sections to the higher-order dynamical terms in U, we have assumed that the neutrons and protons fall off at the same rate in the nuclear surface. While this is not a good assumption in the case of realistic nuclear densities, it does simplify the treatment of second-order terms and allows us to arrive at the semiquantitative understanding we are after.

Now we want to evaluate $F^{(0+)}$ and $F^{(-+)}$ in terms of the C and D coefficients. In the resonance region the real part of the phase function $\tilde{\chi}$ is small, so we may regard the D coefficients, which depend on the real part of $\tilde{\chi}$, as a small parameter and omit terms quadratic and higher order in D. Also in what follows we regard $\Delta\rho/\rho$ and ρ/ρ_0 as small parameters.

Consider first P and ΔP. For SCX we evaluate Eqs. (3.5a) and (3.9b) using Eqs. (3.11) and Table II. We find

$$P^{(0+)}=\frac{(2T+1)(T+1)}{4T}\left[\frac{\Delta\rho}{\rho}\right]^2 C_2{}^2\,, \tag{3.15a}$$

$$\Delta P^{(0+)}=0\,, \tag{3.15b}$$

where $\Delta P^{(0+)}$ has been set to zero because it is second order in the small parameters relative to the results of I. For DCX the results are

$$P^{(-+)}=-\frac{(2T+1)(T+1)}{8T}\left[\frac{\Delta\rho}{\rho}\right]^2\times\left[C_1{}^2+C_1C_3\frac{\Delta\rho}{\rho}\left[\frac{T+3}{4T}\right]\right] \tag{3.15c}$$

and

$$\Delta P^{(-+)}=-ka_\rho\frac{(2T+1)(T+1)}{4T}\left[\frac{\Delta\rho}{\rho}\right]^2 C_1D_1\,. \tag{3.15d}$$

The corresponding results for S and ΔS are

$$S^{(0+)}=\frac{(2T+1)(T+1)}{2}\frac{\Delta\rho}{\rho}\left[C_1+\frac{1}{4}\frac{\Delta\rho}{\rho}C_3\right], \tag{3.16a}$$

$$\Delta S^{(0+)}=ka_\rho\frac{(2T+1)(T+1)}{2}\frac{\Delta\rho}{\rho}\left[D_1-\frac{1}{2}\frac{\Delta\rho}{\rho}D_3\right], \tag{3.16b}$$

TABLE II. Differences of $\gamma^{(1)}$, $\gamma^{(1)^2}$, and $\gamma^{(2)}$.

		$\Gamma^{(0)}$	$\Gamma^{(1)}$	$\Gamma^{(2)}$
i	j	$\gamma^{(1)}(i)-\gamma^{(1)}(j)$	$\gamma^{(2)}(i)-\gamma^{(2)}(j)$	$\gamma^{(1)^2}(i)-\gamma^{(1)^2}(j)$
T	$T-1$	$\frac{1}{2}$	$-\frac{1}{2}\left[\frac{2T+3}{2T-1}\right]$	$-\frac{1}{4}\left[\frac{T+2}{T}\right]$
$T+1$	T	$\frac{T+1}{2T}$	$\frac{T+1}{2T}$	$\frac{T^2-1}{4T^2}$
$T+1$	$T-1$	$\frac{2T+1}{2T}$	$-\frac{1}{2T}\left[\frac{2T+1}{2T-1}\right]$	$-\left[\frac{2T+1}{4T^2}\right]$

$$S^{(-+)}=\frac{(2T+1)(T+1)}{8T}\left[\frac{\Delta\rho}{\rho}\right]^2 \times\left[C_3-\frac{8T}{2T-1}\frac{\rho}{\rho_0}C_2-8\frac{\rho}{\rho_0}C_4\right], \quad (3.16c)$$

and

$$\Delta S^{(-+)}=-ka_\rho\frac{(2T+1)(T+1)}{4T}\left[\frac{\Delta\rho}{\rho}\right]^2 \times\left[D_3+\frac{4T}{2T-1}\frac{\rho}{\rho_0}D_2+4\frac{\rho}{\rho_0}D_4\right]. \quad (3.16d)$$

Finally, combining the results in Eqs. (3.11), (3.15), and (3.16) we find for SCX

$$F^{(0+)}(\theta)=\frac{1}{2}\frac{k\bar{R}}{\sqrt{T}}\frac{\Delta\rho}{\rho}a_\rho\left\{J_0(q\bar{R})\left[i\left[C_1+\tfrac{1}{4}C_3\frac{\Delta\rho}{\rho}\right]+D_1-\tfrac{1}{2}D_3\frac{\Delta\rho}{\rho}\right]+\frac{a_\rho}{\bar{R}}[J_0(q\bar{R})-q\bar{R}J_1(q\bar{R})]\left[\frac{A}{ka_\rho}\left[C_1+\frac{1}{4}\frac{\Delta\rho}{\rho}C_3\right]+\frac{i}{2T}C_1{}^2\frac{\Delta\rho}{\rho}\right]\right\}, \quad (3.17a)$$

where

$$\bar{R}=\tfrac{1}{2}(R_T+R_{T-1}) \quad (3.17b)$$

and

$$A=A_{T+1}\,. \quad (3.17c)$$

For DCX we obtain

$$F^{(-+)}(\theta)=-\left[\frac{2T-1}{T}\right]^{1/2}\frac{k\bar{R}}{8T}\left[\frac{\Delta\rho}{\rho}\right]^2 a_\rho\left\{J_0(q\bar{R})\left[i\left[C_3-\frac{8T}{2T-1}C_2\frac{\rho}{\rho_0}-8\frac{\rho}{\rho_0}C_4\right]-2\left[D_3+\frac{4T}{2T-1}D_2\frac{\rho}{\rho_0}+4\frac{\rho}{\rho_0}D_4\right]\right]+\frac{a_\rho}{\bar{R}}[J_0(q\bar{R})-q\bar{R}J_1(q\bar{R})]\left[\frac{A}{ka_\rho}\left[C_3-\frac{8T}{2T-1}c_2\frac{\rho}{\rho_0}-8\frac{\rho}{\rho_0}C_4\right]-i\left[C_1{}^2+C_1C_3\frac{\Delta\rho}{\rho}\left[\frac{T+3}{4T}\right]\right]-2C_1D_1\right]\right\}, \quad (3.18a)$$

$$\bar{R}=\tfrac{1}{2}(R_{T+1}+R_{T-1})\,, \quad (3.18b)$$

and

$$A=A_T\,. \quad (3.18c)$$

These results express the charge exchange amplitudes in a form suitable for studying the sensitivity to the second-order terms in the optical potential, which we do in the next section.

IV. NUMERICAL RESULTS AND DISCUSSION

Our main interest in this paper is to study the effects of the second-order optical potential on single and double charge exchange. In practice, elastic scattering will also be affected by $U^{(2)}$, but to a much lesser extent than charge exchange. The reason is that the location of the diffractive minima of the elastic cross section and the depths of these minima are determined[22] primarily by $U(r)$ near

$r=\bar{R}$, where

$$\rho(\bar{R})/\rho(0)\simeq 0.1 .$$

For a given model of the density, these properties of $d\sigma/d\Omega$ will therefore be most sensitive to the Fermi broadening and energy shift which characterize $U^{(1)}$. However, the isoscalar term in $U^{(2)}$ may have an appreciable effect on the slope of U near $r=\bar{R}$, which determines the height of the secondary maxima of the angular distribution through the Inopin factor [see below Eq. (3.4e)]. Therefore in practice, the energy shift, Fermi broadening, and $\lambda_0^{(2)}$ coefficients will be fixed by elastic scattering; charge exchange will be most useful for determining the remaining $\lambda^{(2)}$ coefficients.

In order to appreciate the sensitivity of SCX and DCX angular distributions to the second-order terms in U, we next show the result of numerical solutions of the Klein-Gordon equation for various choices of the parameters $\lambda^{(2)}$. In Sec. II we gave some general characteristics of the $\lambda^{(2)}$ parameters, which we now use for guidance in our calculations. Because $\lambda^{(2)}$ are presumably strongly energy dependent but weakly dependent on N and Z, we are able to study in some detail the systematics of the nucleus dependence of the SCX and DCX. Some of the results depend on the $\lambda^{(2)}$ parameters in an intricate way, but the results can be easily understood on the basis of the analytic theory. For displaying the sensitivity of the results to the parameters of the second-order potential, we consider ranges bounded by the conditions

$$|\lambda_i^{(2)}| \le |\lambda_i^{(1)}| \text{ for } i=0,1 , \tag{4.1a}$$

$$|\lambda_i^{(2)}| \le |\lambda_0^{(2)}| \text{ for } i=2,4 . \tag{4.1b}$$

Equation (4.1) guarantees that the second-order terms never dominate the linear terms in Eq. (3.1) in nuclei. The magnitudes are also consistent with the model calculations in Ref. 5. We do not investigate the sensitivity to $\lambda_3^{(2)}$ because in realistic situations its effects are probably masked by the term $\lambda_0^{(2)}$ in Eq. (3.1).

In this section we demonstrate the sensitivity to the P-wave terms in U only. The reason is that the amplitudes $F^{(-+)}$ and $F^{(0+)}$ in Eqs. (3.17) and (3.18) depend in the same way on the $\lambda^{(2)}$ and $\bar{\lambda}^{(2)}$, i.e., through the same coefficients C_i and D_i. However, the amplitudes are much more sensitive to $\lambda^{(2)}$ than $\bar{\lambda}^{(2)}$. This is seen in Appendix A [see Eq. (A6)], where it is shown that the former is multiplied by moderately large coefficients which depend on the Laplacian of the nuclear density.

In most examples below, the densities are of Woods-Saxon form with radius parameter $c=1.1A^{1/3}$ and diffuseness $a=0.56$ fm. Unless specifically stated, the proton and neutron shapes will be taken to be the same. This schematic model for the densities it not a realistic choice for charge exchange (see I and Ref. 3), but it is adequate for studying sensitivities to higher-order terms. The $\lambda^{(1)}$ coefficients are obtained from free pion-nucleon scattering as discussed in Sec. II, with a 20-MeV energy shift.

Consider first SCX. We show in Fig. 1 the dependence of the 0° cross section on A for ^{18}O, ^{48}Ca, ^{58}Ni, ^{90}Zr, ^{120}Sn, and ^{208}Pb at $T_\pi=180$ MeV. The results shown are numerical solutions with PIESDEX. The solid curve is the result with no second-order optical potential. The long dashed curve is the result of turning on the second-order isovector interaction with $\lambda_1^{(2)}=0.5\,i\,\mathrm{Im}\lambda_1^{(1)}$. The effect is to increase the 0° cross section uniformly throughout the periodic table. Such an effect is expected from an examination of the coefficient C_1 in Eq. (3.17a), which is the dominant term in the SCX angular distribution. Equation (3.13c) shows that C_1 is determined, essentially, by the ratio of the isovector to isoscalar interaction, $(W_1/W_0)\mathrm{Im}\Lambda_0^{(1)}/W_0$. This ratio is very weakly dependent on the target, because the dependence on the target comes only through ρ/ρ_0 [see Eqs. (3.13g), (3.13h), (A6), and (A9)], $\bar{R}$, and the quantities μ_1, μ_2, and μ_3 [see Eqs. (A10)], which arise from the Wallace corrections. Equation (3.13c) also shows that a decrease in the isoscalar potential should be approximately as effective as increasing the isovector interaction. Indeed, we see by comparing the dotted-dashed curve in Fig. 1 ($\lambda_0^{(2)}=-0.5i\,\mathrm{Im}\lambda_0^{(1)}$ and $\lambda_1^{(2)}=0.5i\,\mathrm{Im}\lambda_1^{(1)}$) to the long-dashed curve that the magnitude of the SCX cross section is somewhat more sensitive to the iso-

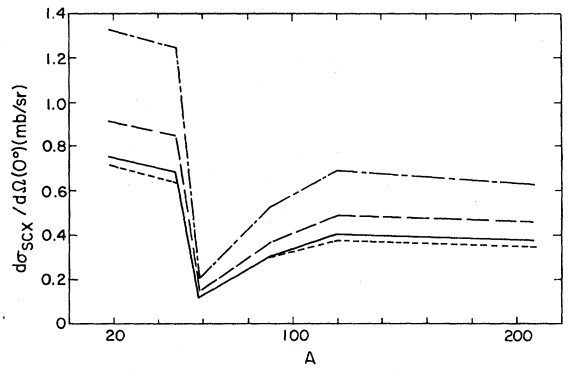

FIG. 1. Angular distribution at 0° for SCX from nuclei throughout the periodic table at 180 MeV obtained with PIESDEX. The solid curve corresponds to no quadratic terms in U. The long-dashed curve is calculated with $\lambda_1^{(2)}=0.5i\,\mathrm{Im}\lambda_1^{(1)}$, the dotted-dashed curve with $\lambda_1^{(2)}=0.5i\,\mathrm{Im}\lambda_1^{(1)}$ and $\lambda_0(2)=-0.5i\,\mathrm{Im}\lambda_0^{(1)}$, and the short-dashed curve with $\lambda_2^{(2)}=i\,\mathrm{Im}\lambda_0^{(1)}$.

scalar than the isovector second-order potential. However, since elastic scattering determines $\lambda_0^{(2)}$, in practice one will not have the freedom to vary $\lambda_0^{(2)}$. To the level of approximation we are considering here, the SCX angular distribution is independent of the isotensor coefficients in U [see Eq. (3.17)], which enter only into C_2 and D_2. The short-dashed curve in Fig. 1 is the PIESDEX solution with $\lambda_2^{(2)}=i\,\mathrm{Im}\lambda_0^{(1)}$, which verifies that SCX is insensitive to this term.

We have chosen to illustrate the sensitivity of the single-charge-exchange cross section to $\lambda_0^{(2)}$ by taking its imaginary part to be opposite in sign to $\mathrm{Im}\lambda_0^{(1)}$. The reason for this choice deserves some comment. In Ref. 5,

$$\mathrm{Im}\lambda_0^{(2)}/\mathrm{Im}\lambda_0^{(1)}$$

was evaluated to be *positive* and large, $\simeq 0.6$. The main contribution to this term arose from the Pauli correction. The Pauli effect is expected to enhance the imaginary part of the isoscalar potential in the vicinity of the resonance because it suppresses the imaginary part of the isobar self-energy. On the other hand, collision broadening terms, which arise from multiple reflections and true absorption, increase the imaginary part of the isobar self-energy and *decrease* the optical potential. The competition between these two effects thus determines the sign of the imaginary part of $\lambda_0^{(2)}$. The density dependence of collision broadening effects was estimated in Ref. 27 using the self-consistent theory of Ref. 25. These results compare favorably to phenomenological determinations[26] of collision broadening. There it was shown that at low density in nuclear matter the optical potential has the behavior

$$U=-4\pi\rho\left[f+g_1\frac{\rho}{\rho_c}\right], \tag{4.2}$$

where f is the free pion-nucleon scattering amplitude, g_1 is a correction, which at 180 MeV is almost purely imaginary and opposite in sign to $\mathrm{Im}f$. The critical density ρ_c is $\rho_0/4\simeq 0.04$ fm^{-3}. Comparing to the notation of Ref. 5 and using the value of g_1 in Table I of Ref. 27 we deduce

$$\frac{\mathrm{Im}\lambda_0^{(2)}}{\mathrm{Im}\lambda_0^{(1)}}\ (\text{collision broadening})\simeq\frac{\mathrm{Im}g_1\rho_0}{\mathrm{Im}f\rho_c}\simeq -1.07\ . \tag{4.3}$$

Thus, the net effect of collision broadening plus Pauli principle would give

$$\mathrm{Im}\lambda_0^{(2)}/\mathrm{Im}\lambda_0^{(1)}\simeq -0.4\ , \tag{4.4}$$

which is close to our actual choice.

We have remarked that the C and D coefficients in Eq. (3.17) are weakly dependent on the target mass. For a given Z the dependence of the cross section on $N-Z$ is displayed explicitly in Eq. (3.17) through $\Delta\rho/\rho$ and T. The major variation arises from the leading (geometrical) factors

$$\frac{\Delta\rho}{\rho}\frac{1}{\sqrt{T}}\ .$$

Thus, the *magnitude of the cross section of SCX depends on having the correct amount of second-order effect,* but the *variation of the cross section throughout an isotopic series reflects most strongly the geometrical aspects of the nucleus,* i.e., the neutron and proton distributions. This aspect of the scattering has been verified experimentally.[3] The most significant correction to the dependence on $N-Z$ is the term C_3 in Eq. (3.17). To obtain the correct ratio of C_1 to C_3 it is necessary to know both the isoscalar and isovector interactions separately, but the sensitivity of the cross section to C_3 is weak due to the fact that it is multiplied by

$$\frac{1}{4}\frac{\Delta\rho}{\rho}\ .$$

To determine empirically the isoscalar and isovector terms, careful phenomenological studies of both elastic and SCX scattering are needed.

Consider next the variation of the zero degree angular distribution for DCX throughout the periodic table. In our schematic model we can understand the numerical results in terms of the analytic theory of Sec. III by dropping terms in the amplitude [Eq. (3.18a)] proportional to a/R and D_i and taking

$$\Delta\rho/\rho=(N-Z)/A\ .$$

Retaining the remaining second-order coefficients, we find

$$\frac{d\sigma}{d\Omega}\mathrm{DCX}(0^\circ)=\sigma_2\frac{(N-Z)(N-Z-1)}{A^{10/3}}\times\left[1+\eta-\frac{4\gamma(N-Z)}{N-Z-1}\right]^2, \tag{4.5}$$

where

$$\eta=8\frac{C_4}{C_3}\frac{\rho}{\rho_0}\ , \tag{4.6a}$$

$$\gamma=\frac{C_2}{C_3}\frac{\rho}{\rho_0}\ . \tag{4.6b}$$

We show in Fig. 2 the 0° cross section at 180 MeV as calculated by PIESDEX for the same set of nuclei as shown in Fig. 1. The solid curve is calculated with the second-order potential set equal to zero,

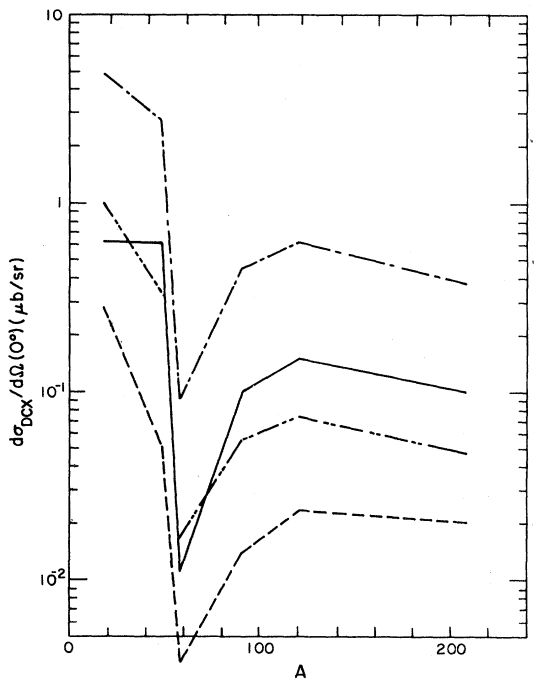

FIG. 2. Angular distribution at 0° for DCX from nuclei throughout the periodic table at 180 MeV obtained with PIESDEX. The solid curve corresponds to no quadratic terms in U. The double-dotted-dashed curve contains the isotensor potential given in Eq. (4.7). The dotted-dashed curve corresponds to the isotensor potential of Eq. (4.7) and in addition $\lambda_1^{(2)}=0.5i\ \mathrm{Im}\lambda_1^{(1)}$, and $\lambda_0^{(2)}=-0.5i\ \mathrm{Im}\lambda_0^{(1)}$. The dashed curve corresponds to the isotensor potential of Eq. (4.2) and in addition $\Delta\lambda_2^{(2)}=0.5i\ \mathrm{Im}\lambda_0^{(1)}$.

and therefore corresponds to the theory of I and may be described by Eq. (4.5) setting $\gamma=\eta=0$. In contrast to SCX, the DCX cross section depends sensitively on the isotensor terms of U. According to Eq. (2.5c) there are two parameters characterizing this component. The parameter $\lambda_2^{(2)}$, which contains among other things the sequential scattering of the pion from two correlated nucleons, enters into the DCX amplitude in Eq. (3.18a) through C_2. The sequential process includes all nonanalog intermediate states as well as the single analog route. To prevent double counting[5] of the single analog route, the coefficient $\lambda_4^{(2)}$ subtracts the iteration of the lowest-order optical potential, implying[28] $\eta\simeq-1$ in Eq. (4.5). For our numerical examples we choose $\lambda_4^{(2)}$ to be fixed by the model of Ref. 5. Including the 20-MeV energy shift, we evaluate

$$\lambda_4^{(2)}=3.0+4.5i\ \mathrm{fm}^3\ . \tag{4.7a}$$

The double dotted-dashed curve in Fig. 2 shows the change from the lowest-order calculation (solid line) by adding the isotensor term $\lambda_4^{(2)}$ as given in Eq. (4.2a) and

$$\lambda_2^{(2)}=-3.0-6.2i\ \mathrm{fm}^3\ , \tag{4.7b}$$

which contains only the direct and exchange pieces of the sequential scattering process as determined in Ref. 5. Note that the effect of the isotensor interaction is to modify significantly the lowest-order calculation. With $\lambda_4^{(2)}$ properly chosen, the rate of fall-off of the DCX cross section is *faster* than that given by the lowest-order calculation by the factor

$$\left[\frac{N-Z}{N-Z-1}\right]^2\ ,$$

consistent with the double dotted-dashed curve in Fig. 2. The net effect of the $\lambda^{(2)}$ in Eqs. (4.2) is to increase the DCX cross section ^{18}O and ^{58}Ni by about a factor of 2 and to decrease the cross section in nuclei with a large neutron excess.

The dashed curve in Fig. 2 shows the effect of changing $\lambda_2^{(2)}$ according to

$$\lambda_2^{(2)}\rightarrow-3.0-6.2i\ \mathrm{fm}^3+\Delta\lambda_2^{(2)}\ , \tag{4.8a}$$

where we take

$$\Delta\lambda_2^{(2)}=i\ \mathrm{Im}\lambda_0^{(1)}\ . \tag{4.8b}$$

We see that there is a uniform decrease in the forward angular distribution throughout the periodic table. The reason for this is that at resonance $\mathrm{Im}\lambda_0^{(1)}$ is positive leading to a reduction of η in Eq. (4.5). Note that once $\lambda_4^{(2)}$ has been fixed, further variation in the isotensor potential through changes in $\lambda_2^{(2)}$ do not affect the relative magnitudes of the zero-degree cross sections.

Consider next the effect of an isoscalar and isovector second-order potential in addition to the isotensor terms of Eq. (4.7). By taking $\lambda_1^{(2)}=0.5i\ \mathrm{Im}\lambda_1^{(1)}$ and $\lambda_0^{(2)}=-0.5i\ \mathrm{Im}\lambda_0^{(1)}$, we obtain the result given by the dotted-dashed curve in Fig. 2. As compared to the calculation without $\lambda_0^{(2)}$ and $\lambda_1^{(2)}$ (double-dotted-dashed), there is a uniform upward shift by about a factor of 5. To understand the effect of the second-order isovector and isoscalar terms in the analytic model we must study the term C_3 in Eq. (3.18a), which is given in Eq. (3.13e). The dominant term is $(W_1/W_0)^2\mathrm{Im}\Lambda_0^{(1)}/W_0$, which is a number close to 1 at resonance and in the absence of second-order terms. The fact that this is quadratic in the ratio of isovector to isoscalar potentials is the reason why DCX is so much more sensitive to the second-order effects than is SCX. The increase throughout the periodic table is uniform because the terms contributing to C_3 do not have a strong dependence on the nuclear mass, for the same

reasons discussed in connection with the sensitivity of SCX to isoscalar and isovector second-order terms.

To summarize, the *shape* of the A and T dependence of the zero degree $d\sigma/d\Omega$ for DCX is relatively insensitive to the amount of second-order optical potential, once the correction for the nonanalog route in the sequential process has been applied. The overall scale for the variation is set by the relative amount of $\lambda_0^{(2)}$, $\lambda_1^{(2)}$, *and* $\lambda_2^{(2)}$. The interplay between those terms can be quite intricate, but the net result is easily understood in terms of the analytic theory.

Figure 3 shows angular distributions for DCX from ^{18}O at $T_\pi = 180$ MeV that result from calculations with PIESDEX. The solid curve corresponds to the case of all $\lambda^{(2)}$ coefficients of Eq. (2.5) set equal to zero and is therefore what one would calculate from the lowest-order optical potential. The double-dotted-dashed curve corresponds, in addition to the lowest-order potential, to including the isotensor potential of Eqs. (4.7) and (4.8) with $\Delta\lambda_2^{(2)}=0$. The magnitude of the 0° cross section has increased by about a factor of 2, in accordance with the calculation in Fig. 2, but the shape of the cross section

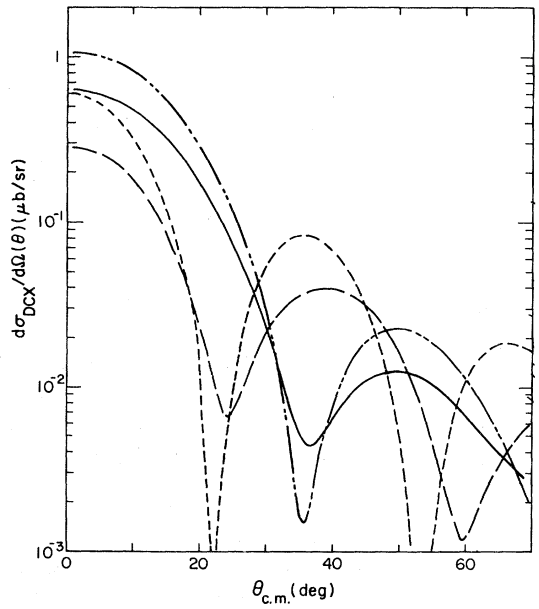

FIG. 3. Angular distributions for DCX on ^{18}O at 180 MeV obtained with PIESDEX. The solid curve corresponds to no quadratic terms in U. The double-dotted-dashed curve contains the isotensor potential given in Eq. (4.7). The long-dashed curve contains, in addition, $\Delta\lambda_2^{(2)} = i\,\mathrm{Im}\lambda_0^{(1)}$. The short-dashed curve is obtained by using the more realistic valence neutron wave functions of Ref. 29 and the isotensor potential used for the long-dashed curve.

remains unchanged except for an enhancement of its diffractive character. The long-dashed curve corresponds to the choice $\Delta\lambda_2^{(2)} = i\,\mathrm{Im}\lambda_0^{(1)}$. Note that the magnitude of the 0° cross section has decreased and that the position of the first minimum has moved to smaller angles by nearly 12°, to 24°. The short-dashed curve results from using a more realistic description of the valence neutrons than our schematic model in which the proton and neutron densities have the same shape. For this calculation we kept the $\lambda^{(2)}$ parameters fixed to the values used for the long-dashed curve, but now, in accordance with the discussion in Sec. I, we take $\Delta\rho = \rho_{\mathrm{val}}$, where ρ_{val} is the valence neutron density calculated from the valence neutron wave functions of Negele and Vautherin.[29]

The sensitivity of the shape of the DCX angular distribution to $\Delta\lambda_2^{(2)}$ can be easily understood from the analytic results in Eqs. (3.13) and (3.18a). When $\lambda_2^{(2)} \simeq 0$, the cancellation implied by $\eta = -1$ discussed in connection with Fig. 2 suppresses the contribution of $J_0(qR)$ relative to $J_0(qR) - qRJ_1(qR)$. The former function has a zero near 40° and dominates the solid curve in Fig. 3. The latter function has its first zero near 20°, and the shift of the minimum of the dashed curve in Fig. 3 reflects the increased importance of this term. For the value of $\Delta\lambda_2^{(2)}$ corresponding to the dashed curve, the coefficient of $J_0(qR)$ is negative, causing $J_0(qR)$ to add in coherently at larger angles with the consequence that the position of the minimum is shifted to a smaller angle, $\theta_{\mathrm{min}} \simeq 24°$. The isotensor term in U affects the $J_0(qR)$ term differently from the term $J_0(qR) - qRJ_1(qR)$ because it has a different range from the iterated lowest-order optical potential. Thus, the shifting of the minimum is due to an interference between two amplitudes of different ranges: (1) the second-order isotensor potential and (2) the iteration of the lowest-order optical potential to *all* orders. As suggested by all analytic results, the magnitude of the zero degree cross section can be scaled by appropriate choice of $\lambda_0^{(2)}$, $\lambda_1^{(2)}$, and $\lambda_2^{(2)}$ while maintaining minimum at a given angle.

To obtain a feeling for the extent of validity of the analytic theory when second-order effects are included, we have compared the results in Eqs. (3.13), (3.14), (3.17), and (3.18), and Appendix A to the corresponding solution of the Klein-Gordon equation. We have found that the analytic theory faithfully reproduces the sensitivity of the exact calculations to variations of the parameters of $U^{(2)}$, but does not reproduce the absolute magnitude of the cross sections. The degree of discrepancy in the magnitude over the energy range 130—190 MeV is roughly the same as shown in Figs. 4(a) and (b). These figures give the angular distributions for 180 MeV SCX and

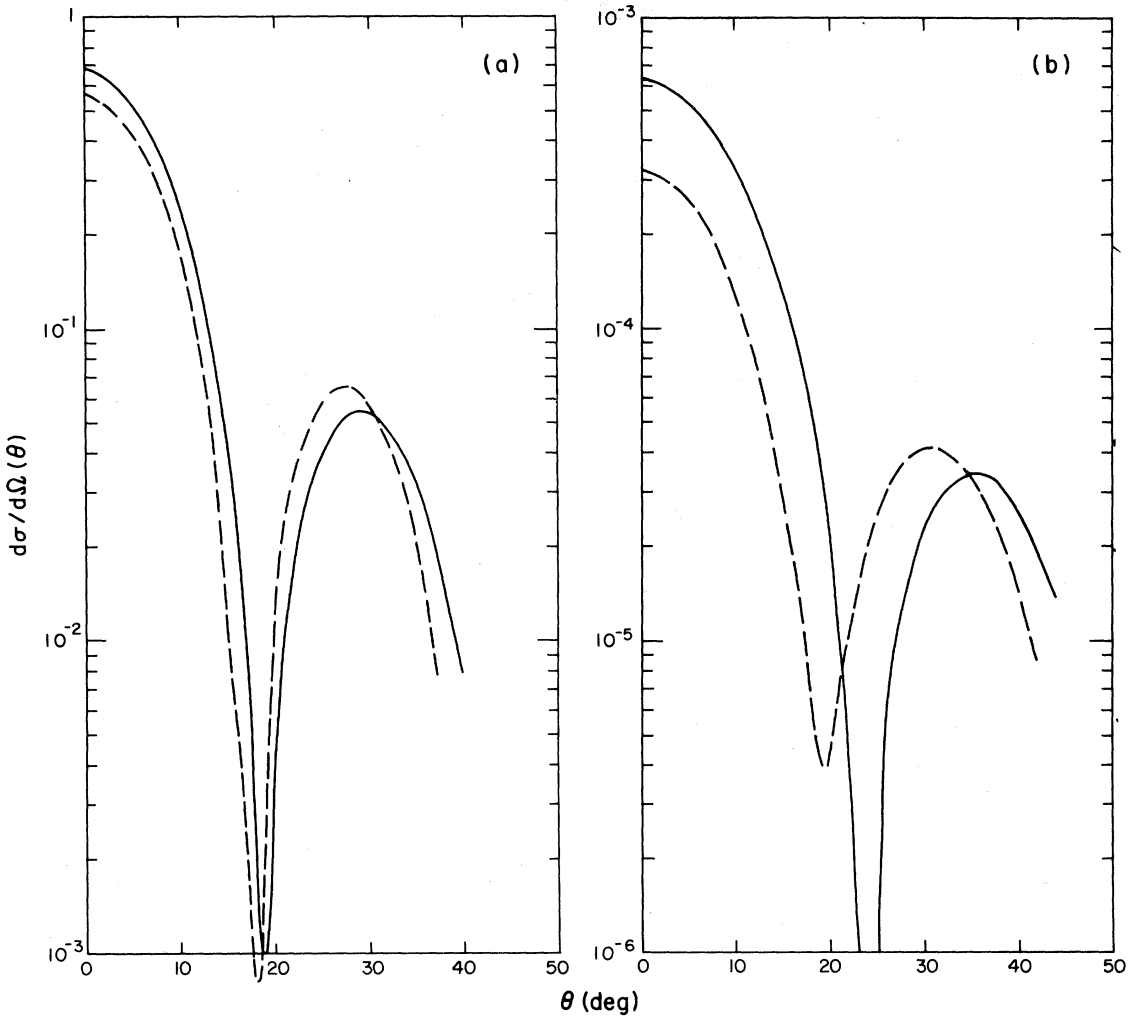

FIG. 4. Comparison of analytic angular distributions (dashed curves) to PIESDEX results (solid curves) for SCX on ^{48}Ca [part (a)], and for DCX on ^{48}Ca [part (b)] at 180 MeV. Units are mb/sr.

DCX from ^{48}Ca with the $\lambda^{(2)}$ parameters set to zero. In these figures, the solid curves are the results of PIESDEX calculations and the dashed curves result from the analytic theory. The angular distribution of SCX is shown in Fig. 4(a). Note that the analytic theory is in good agreement with the model exact calculation. The improvement (over the results of I) in the height of the secondary maximum is due to the inclusion of the Inopin factor [see below Eq. (3.4e)], and improvement in the depth of the minimum is the result of a better treatment of Re$\tilde{X}$. For the minimum to occur at the proper location, it is necessary to have the correct diffractive radius $\bar{R}$ as well as the correct linear combination of the Bessel functions $J_0(q\bar{R})$ and $J_0(q\bar{R})-q\bar{R}J_1(q\bar{R})$ in Eqs. (3.17) and (3.18). The result for DCX is shown in Fig. 4(b). Generally speaking, DCX is more sensitive to small corrections than is SCX, and agreement with the computer solution is correspondingly less good than in the case of SCX.

Finally, we remark that because the eikonal theory is a semiquantitative theory, one should use the actual computer solution of the Klein-Gordon equation to calculate cross sections. However, we found that the analytic theory sufficiently accurately reflects the systematics of the underlying optical

model to be useful in understanding our results, and thus we have devoted so much attention to the analytic theory.

V. EXPERIMENTAL IMPLICATIONS AND SUMMARY

Pion elastic scattering, and SCX and DCX scattering to analog states contain two types of information which one would like to be able to determine separately. One is nuclear structure and the other pion- and isobar-nucleus reaction dynamics.

In order to use charge exchange reactions to probe this information, it is necessary that the distinction between nuclear structure and reaction dynamics be clearly made in the optical potential. This distinction is manifest in the form chosen in Eq. (2.5), in which the reaction dynamics is contained entirely in the parameters $\lambda^{(1)}$ and $\lambda^{(2)}$. We demonstrated in Sec. IV using our schematic model that the reaction dynamics and nuclear structure information manifest themselves differently in the cross sections. In particular, the relative magnitudes of the zero degree cross sections are dominated by the geometrical properties of the nucleus, i.e., the valence neutron density $\Delta\rho$ and the target isospin T. The reaction dynamics, on the other hand, determines primarily the overall scale, which involves an intricate interplay between the $\lambda_0^{(2)}$ (isoscalar) and $\lambda_1^{(2)}$ (isovector) coefficient for SCX and in addition the $\lambda_2^{(2)}$ (isotensor) coefficient for DCX. At the present time, the valence neutron densities are probably better known than the reaction theory, so that one can test this prediction by comparing the relative magnitudes of the theoretical cross sections calculated from realistic densities to experiment. If these predictions are verified, one will then presumably also obtain a significant measure of the reaction dynamics through the value of the overall scale factors. Eventually, the charge exchange measurements may provide a means for studying experimentally the neutron halo in detail. In this section, we are concerned with calculating from our theory the relative zero degree cross sections using DME densities[29] and also with comparing these results to the schematic model of Sec. V.

Consider first the location of the minimum of the differential cross section for double charge exchange from ^{18}O. The experimental angular distribution[30–33] is anomalous in that the position of the first minimum occurs at $\theta_{\min}\simeq 22°$, whereas most theoretical calculations with lowest-order U give $\theta_{\min}\simeq 35°$–$40°$. In a theory that includes the isotensor interaction, such a shift can occur naturally as a consequence of the reaction dynamics. It was shown explicitly in Sec. IV that the minimum can move, in a direction to agree with experiment, as a result of an interference of two amplitudes of slightly different ranges. The fact that a strong interference occurs between a relatively well-known component of the interaction and a relatively poorly known isotensor term means that the angular distribution gives a clean measure of the sign and magnitude of $\lambda_2^{(2)}$. In our theory this interference occurs through a contribution $\Delta\lambda_2^{(2)}$ to $\lambda_2^{(2)}$ such that $\mathrm{Im}\Delta\lambda_2^{(2)}$ has the *same* sign as $\mathrm{Im}\lambda_0^{(1)}$. Our results in Fig. 3 of Ref. 5 give an isotensor interaction of the opposite sign to this, and therefore we can exclude the Pauli principle and the excitation of nonanalog intermediate states as explanations. Other possibilities include interactions with the spin density of ^{18}O and interactions of isobars with the nucleus, which are now under investigation. There may be many other possibilities, but we emphasize that our theory requires the phase and magnitude of $\mathrm{Im}\Delta\lambda_2^{(2)}$ be such that [see Eq. (4.3b)] $\mathrm{Im}\Delta\lambda_2^{(2)}/\mathrm{Im}\lambda_0^{(1)}\simeq 1$. With this value of $\Delta\lambda_2^{(2)}$, the angular distribution shown in Fig. 3 (short-dashed curve) has a shape very similar to the experimental data at 164 MeV.[32,33] Although the curve shown is a factor of 2 below the data, we remind the reader that the cross section is easily scaled upward without a change in shape by an appropriate choice of $\lambda_0^{(2)}$, $\lambda_1^{(2)}$, and $\lambda_2^{(2)}$. An example of a fit to the data by adjusting these parameters appears elsewhere.[34] By comparing the short-dashed and long-dashed curves in Fig. 3, we see that the effect of using realistic densities is to increase the overall magnitude of the cross section without appreciably affecting the shape. Similar effects of adding an isotensor potential were recently reported by Liu.[35]

Consider next the zero-degree cross sections for SCX and DCX throughout the periodic table at 180 MeV. We show in Tables III and IV the results of three calculations with PIESDEX, each including the lowest-order potential described in Sec. I. Otherwise the calculations correspond to: (a) the schematic model with no isotensor potential, (b) the schematic model with $\lambda_2^{(2)}$ and $\lambda_4^{(2)}$ from Eqs. (4.7a) and (4.7b), and (c) DME densities[29] with the isotensor potential from Eqs. (4.7a) and (4.7b).

From these tables, the following points are to be observed. The results for SCX in the schematic model scale as $(N-Z)A^{-10/3}$, as expected from the results of I (see column 1 of Table IV). It is amusing that the results of calculation (c) with realistic densities also scale in approximately the same way (see column 2 of Table IV). The overall scale factor is different, however, reflecting the fact that for realistic densities $\Delta\rho/\rho > (N-Z)/A$ for most cases. In cases where comparison to experiment is possible, it is found that the experiment follows the law $(N-Z)A^{-4/3}$, but that the scale is about a factor of

TABLE III. Zero degree SCX and DCX differential cross sections at 180 MeV as calculated with PIESDEX.

Target	SCX[a] (mb/sr)	DCX[a] (μb/sr)	SCX[b] (mb/sr)	DCX[b] (μb/sr)	SCX[c] (mb/sr)	DCX[c] (μb/sr)
^{18}O	0.751	0.631	0.731	1.02	1.84	1.86
^{26}Mg	0.423	0.187	0.416	0.296	0.694	0.581
^{42}Ca	0.195	0.035	0.193	0.055	0.598	0.236
^{48}Ca	0.679	0.622	0.652	0.339	1.73	1.29
^{58}Ni	0.116	0.011	0.115	0.017	0.603	1.03
^{90}Zr	0.301	0.102	0.294	0.055	0.843	0.317
^{120}Sn	0.395	0.151	0.381	0.074	1.64	0.595
^{208}Pb	0.366	0.103	0.349	0.048	1.58	0.514

[a]Schematic model for ρ_{val}, $\lambda_2^{(2)}=\lambda_4^{(2)}=0$.
[b]Schematic model for ρ_{val}, $\lambda_4^{(2)}$, and $\lambda_2^{(2)}$ from Eq. (4.7).
[c]DME model for ρ_{val}, $\lambda_2^{(2)}$, and $\lambda_4^{(2)}$ from Eq. (4.7).

2 greater than that given by the lowest-order theory. We saw in Sec. IV that if $\text{Im}\lambda_0^{(2)}/\text{Im}\lambda_0^{(1)}<0$ and $\text{Im}\lambda_1^{(2)}/\text{Im}\lambda_1^{(1)}>0$, then the scale factor may be increased. We have seen that a combination of collision broadening and the Pauli principle gives a second-order potential with these properties, but until a more detailed theoretical analysis of these and other second-order processes, one cannot say with certainty that the reaction dynamics is understood theoretically.

In the case of double charge exchange, we note from column 3 of Table IV that the schematic model with no isotensor potential scales (approximately) as $(N-Z)(N-Z-1)A^{-10/3}$, which is expected from I. When the isotensor potential is added, this law is violated, as can be verified by comparing columns 4 and 5 of Table IV. The reasons for this were discussed in detail in Sec. V. We reiterate that the physics of the additional dependence on $(N-Z)$ arises from careful consideration of the nonanalog intermediate states in DCX. These effects have been studied in Ref. 36 for $^{18}\text{O}(\pi^+,\pi^-)^{18}\text{Ne}$, and our findings are consistent with this paper.

Finally, we consider the effect of using realistic densities for DCX, shown in the last column of Table III. Remarkably, these results scale to within factors of 2 as $(N-Z)(N-Z-1)A^{-10/3}$, except for the case of ^{58}Ni and ^{42}Ca. One should not conclude that the physics is uninteresting just because a relatively simple formula parametrizes the results. We also point out that the magnitudes of the cross sections for ^{18}O, ^{26}Mg, ^{42}Ca, and ^{48}Ca fall very close to the measurements as quoted in Ref. 30. As emphasized in Ref. 30, it has been difficult to understand the ratio of DCX in ^{42}Ca compared to ^{48}Ca in models without an isotensor interaction, but in our model the ratio is 5.4, which is the same as the measurement.[37] This ratio has been interpreted in Ref. 38 as an effect of an interference between an analog and nonanalog amplitude in DCX in a less explicit model than ours.

Preliminary comparisons have shown that our theory agrees favorably with the experimental data on the relative variation of the zero-degree cross section for SCX and DCX throughout the periodic table. If these results are upheld when more com-

TABLE IV. Various ratios of zero degree cross sections given in Table III.

Target	$\frac{\text{SCX}^a}{(N-Z)A^{-4/3}}$	$\frac{\text{SCX}^c}{(N-Z)a^{-4/3}}$	$\frac{\text{DCX}^a/10^3}{(N-Z)(N-Z-1)A^{-10/3}}$	$\frac{\text{DCX}^a}{\sigma(^{18}\text{O})}$	$\frac{\text{DCX}^b}{\sigma(^{18}\text{O})}$	$\frac{\text{DCX}^c}{\sigma(^{18}\text{O})}$
^{18}O	17.9	43.4	4.82	1	1	1
^{26}Mg	16.3	26.7	4.87	0.296	0.290	0.312
^{42}Ca	13.3	43.7	4.51	0.055	0.054	0.127
^{48}Ca	14.8	37.7	4.46	0.986	0.332	0.694
^{58}Ni	12.9	67.7	4.15	0.017	0.017	0.554
^{90}Zr	12.0	34.0	3.70	0.162	0.054	0.170
^{120}Sr	11.6	48.5	3.39	0.239	0.073	0.320
^{208}Pb	10.2	44.3	2.90	0.163	0.047	0.276

plete sets of data become available, we will have an empirical confirmation of the separation between nuclear structure and reaction dynamics given in Eq. (2.2) for U. We can then determine the $\lambda^{(2)}$ parameters from the absolute magnitude of the cross sections. Elastic scattering and SCX determine the isoscalar and isovector parameters $\lambda_0^{(2)}$ and $\lambda_1^{(2)}$. Our results suggest that these would increase the DCX cross sections above those given in Table III. However, the experimental angular distribution for $^{18}O(\pi^+,\pi^-)^{18}Ne$ requires that a large isotensor potential $\Delta\lambda_2^{(2)}$ is also needed and the sign is such to uniformly scale the zero-degree cross sections back down. Thus, this choice of parameters would achieve a consistency between the measurements of zero-degree cross sections for SCX and DCX and the DCX angular distribution for $^{18}O(\pi^+,\pi^-)^{18}Ne$. Detailed comparisons between experiment and theory will be made in a subsequent publication. Angular distributions for DCX on a variety of elements of various isospin at 164 MeV would be helpful in confirming the ideas suggested here.

This work was supported by the U. S. Department of Energy.

APPENDIX A: EXPLICIT EXPRESSIONS FOR $\tilde{\Lambda}^{(2)}$ COEFFICIENTS

Given the form of the optical potential defined by Eq. (2.6), we follow the procedure outlined in Appendix B of I to obtain a phase shift equivalent local potential for each total isospin channel

$$U=\frac{-1}{1-\xi}\left[k^2\bar{\xi}+k^2\xi+\frac{p}{2}\nabla^2\xi\right]+\frac{(\xi')^2}{4(1+\xi)^2}\ . \tag{A1a}$$

The transformation used to obtain Eq. (A1) is well defined provided $\xi\neq 1$. In addition to this condition, we will also assume that we may expand Eq. (A1) in powers of ξ

$$U=\sum_{n=1}^{\infty}u^{(n)}(\xi,\bar{\xi})\ . \tag{A2}$$

By using the binomial expansion we obtain

$$k^{-2}u^{(n)}(\xi,\bar{\xi})=-\left[\bar{\xi}\xi^{n-1}+\xi^n+\frac{\xi^{n-1}}{2k^2}p\nabla^2\xi-\frac{n-1}{4k^2}(\xi')^2\xi^{n-2}\right]\ . \tag{A3}$$

We are interested here in terms up to order ρ^2, and therefore only the terms $u^{(1)}$ and $u^{(2)}$ will be needed. Furthermore, ξ has terms linear and quadratic in density, which we make explicit by letting $\xi\to\xi+\Delta\xi$, where now ξ has all terms linear and $\Delta\xi$ all terms quadratic in density. Therefore, through order ρ^2 we obtain from Eqs. (A2) and (A3)

$$U(\xi+\Delta\xi,\bar{\xi}+\Delta\bar{\xi})\simeq u^{(1)}(\xi,\bar{\xi})+u^{(1)}(\Delta\xi,\Delta\bar{\xi})+u^{(2)}(\xi,\bar{\xi})\ , \tag{A4}$$

and we see that the terms quadratic in the density are due to $u^{(1)}(\Delta\xi)$ and $u^{(2)}(\xi)$. We shall refer to those terms resulting from $u^{(1)}(\Delta\xi)$ as *dynamical* contributions, whereas those resulting from $u^{(2)}(\xi)$ are *geometrical* contributions. Using Eq. (A3), making use of the definition of p [see Eq. (2.6)], we find

$$k^{-2}u^{(1)}(\xi,\bar{\xi})=-[\bar{\xi}+\xi\hat{F}_1\xi]\ , \tag{A5a}$$

$$k^{-2}u^{(2)}(\xi,\bar{\xi})=-[\xi\bar{\xi}+\xi^2\hat{F}_1\xi^2+(1-2p_1)(\xi')^2]\ , \tag{A5b}$$

$$k^{-2}u^{(1)}(\Delta\xi,\Delta\bar{\xi})=-[\Delta\bar{\xi}+\Delta\xi\hat{F}_2\Delta\xi]\ , \tag{A5c}$$

where if f is an arbitrary function

$$\hat{F}_i f=1+\frac{p_i}{2k^2}\frac{\nabla^2 f}{f}\ . \tag{A5d}$$

By using the expressions for ξ and $\Delta\xi$ given in Eqs. (2.6b) and (2.6c), and assuming similar forms for $\bar{\xi}$ and $\Delta\xi$, we have

$$k^{-2}u^{(1)}(\xi,\bar{\xi})=\Lambda_0^{(1)}\rho(1)+\gamma^{(1)}\Lambda_1^{(1)}\rho(2)\ , \tag{A6a}$$

$$k^{-1}u^{(1)}(\Delta\xi,\Delta\bar{\xi})=\Lambda_{0d}^{(2)}\rho(3)+\gamma^{(1)}\Lambda_{1d}^{(2)}\rho(4)+\gamma^{(2)}\Lambda_{2d}^{(2)}\rho(5)+\gamma^{(4)}\Lambda_{4d}^{(2)}\rho(5)\ , \tag{A6b}$$

$$k^{-2}u^{(2)}(\xi,\bar{\xi})=\Lambda_{0g}^{(2)}\rho(3)+\gamma^{(1)}\Lambda_{1g}^{(2)}\rho(4)+(\gamma^{(1)})^2\Lambda_{5g}^{(2)}\rho(5)\ , \tag{A6c}$$

where we have defined, respectively, for $i=1, 2, 3, 4$, and 5

$$\rho(i)=\rho,\ \Delta\rho,\ \frac{\rho^2}{\rho_0},\ \frac{\rho\Delta\rho}{\rho_0},\ \text{and}\ \frac{\Delta\rho^2}{\rho_0}\ , \tag{A6d}$$

$$\Lambda_i^{(1)}\equiv-[\bar{\lambda}_i^{(1)}+\lambda_i^{(1)}\hat{F}_1\rho(i)]\ \text{for}\ i=1,2\ , \tag{A6e}$$

$$\Lambda_{id}^{(2)}\equiv-[\bar{\lambda}_i^{(2)}+\lambda_i^{(2)}\hat{F}_2\rho(i)]\ \text{for}\ i=1,2,4\ , \tag{A6f}$$

$$\Lambda_{0d}^{(2)}\equiv-[\bar{\lambda}_0^{(2)}+\bar{\lambda}_3^{(2)}\rho(5)/\rho(3)+\lambda_0^{(2)}\hat{F}_2\rho(3)+\lambda_3^{(2)}\hat{F}_2\rho(5)]\ , \tag{A6g}$$

$$\Lambda_{0g}^{(2)}\equiv-\rho_0[\bar{\lambda}_0^{(1)}\lambda_0^{(1)}+(\lambda_0^{(1)})^2\hat{F}_3(\rho\rho)]\ , \tag{A6h}$$

$$\Lambda_{1g}^{(2)}\equiv-\rho_0[\bar{\lambda}_0^{(1)}\lambda_1^{(1)}+\bar{\lambda}_1^{(1)}\lambda_0^{(1)}+2\lambda_0^{(1)}\lambda_1^{(1)}\hat{F}_3(\rho\Delta\rho)]\ , \tag{A6i}$$

$$\Lambda_{5g}^{(2)}=-\rho_0[\bar{\lambda}_1^{(1)}\lambda_1^{(1)}+(\lambda_1^{(1)})^2\hat{F}_3(\Delta\rho\Delta\rho)]\ , \tag{A6j}$$

where

$$\hat{F}_3(\rho_a\rho_b)=\left[1+\frac{p_1}{4k^2}\frac{\nabla^2\rho_a\rho_b}{\rho_a\rho_b}\right]+\left[\frac{1-2p_1}{4k^2}\right]\left[\frac{\rho_a'\rho_b'}{\rho_a\rho_b}\right]\ . \tag{A6k}$$

Next, we insert the potential given in Eqs. (A4) and (A6) into the following expression for the eikonal phase

$$\tilde{\chi}(b)=\frac{1}{2k}\int_{-\infty}^{\infty}dz\left[U+\frac{B}{4k^2}U^2\right]\ , \tag{A7a}$$

where

$$B=1+\frac{b^2}{r^2}\frac{d}{dr}=1+\frac{b^2}{Z}\frac{\partial}{\partial Z}\ . \tag{A7b}$$

We obtain

$$\tilde{\chi}(b)\simeq\tilde{\chi}^{(1)}+\tilde{\chi}_0^{(2)}+\gamma^{(1)}\tilde{\chi}_1^{(2)}+\gamma^{(2)}\tilde{\chi}_2^{(2)}+\gamma^{(4)}\tilde{\chi}_4^{(2)}+(\gamma^{(1)})^2\tilde{\chi}_5^{(2)}\ , \tag{A8a}$$

where

$$\tilde{\chi}^{(1)}=k(2\pi ab)^{1/2}\left[\Lambda_0^{(1)}+\Lambda_1^{(1)}\frac{\Delta\rho}{\rho}\right]\rho(b)\ , \tag{A8b}$$

$$\tilde{\chi}_i^{(2)}=k(2\pi ab)^{1/2}\frac{\rho^{2-i}(\Delta\rho)^i}{\rho_0}\tilde{\Lambda}_i^{(2)}\ \text{for}\ i=0,1,2\ , \tag{A8c}$$

$$\tilde{\chi}_4^{(2)}=k(2\pi ab)^{1/2}\frac{(\Delta\rho)^2}{\rho_0}\tilde{\Lambda}_4^{(2)}\ , \tag{A8d}$$

$$\tilde{\chi}_5^{(2)}=k(2\pi ab)^{1/2}\frac{(\Delta\rho)^2}{\rho_0}\tilde{\Lambda}_5^{(2)}\ , \tag{A8e}$$

with

$$\tilde{\Lambda}_0^{(2)}=\Lambda_0^{(2)}X-\frac{1}{\sqrt{2}}\left[(\Lambda_0^{(1)})^2\mu_1-(\Lambda_0^{(2)})^2\mu_3\frac{\rho^2}{\rho_0^2}\right]\ , \tag{A9a}$$

$$\tilde{\Lambda}_1^{(2)}=\Lambda_1^{(2)}X-\frac{2}{\sqrt{2}}\Lambda_1^{(1)}\left[\Lambda_0^{(1)}\mu_1+\Lambda_0^{(2)}\mu_2\frac{\rho}{\rho_0}\right]\ , \tag{A9b}$$

$$\tilde{\Lambda}_2^{(2)}=\Lambda_{2d}^{(2)}X\ , \tag{A9c}$$

$$\tilde{\Lambda}_4^{(2)}=\Lambda_{4d}^{(2)}X\ , \tag{A9d}$$

$$\tilde{\Lambda}_5^{(2)}=\tilde{\Lambda}_{5g}^{(2)}X-\frac{1}{\sqrt{2}}(\Lambda_1^{(1)})^2\mu_1-\frac{1}{\sqrt{2}}\Lambda_1^{(2)}\times\left[2\Lambda_1^{(1)}\mu_2+\Lambda_1^{(2)}\mu_3\frac{\rho}{\rho_0}\right]\frac{\rho}{\rho_0}\ , \tag{A9e}$$

and

$$X=\frac{1}{\sqrt{2}}\left[1-2\left[\Lambda_0^{(1)}\mu_2+\Lambda_0^{(2)}\mu_3\frac{\rho}{\rho_0}\right]\frac{\rho}{\rho_0}\right]\ , \tag{A10a}$$

and

$$\mu_{m-1}=\frac{\rho_0}{4}\left[\frac{2}{m}\right]^{1/2}\left[\frac{mb}{a}-1\right]\ . \tag{A10b}$$

In Eq. (A9) we have used

$$\Lambda_i^{(2)}\equiv\Lambda_{id}^{(2)}+\Lambda_{ig}^{(2)}$$

for $i=0,1$. We have further used the approximation[22]

$$\rho(r)\simeq\rho(b)\exp\left[\frac{-z^2}{2ab}\right]\ , \tag{A11}$$

and employed the integrals

$$\int_{-\infty}^{\infty}dz\,\rho^m(r)=2\rho^m(b)(2\pi ab/m)^{1/2}\ , \tag{A12a}$$

$$\int_{-\infty}^{\infty}dz\left[\frac{b^2}{z}\frac{\partial}{\partial z}\rho^m(r)\right]=-2\rho^m(b)\frac{bm}{a}(2\pi ab/m)^{1/2}\ , \tag{A12b}$$

to do the integral in Eq. (3.7) with Eqs. (A4)—(A6).

APPENDIX B: DETAILS ON DETERMINING DEPENDENCE OF F_τ ON A_τ

We extend Eq. (22) of I by writing the expansion of F about $\bar{A}$ and $\bar{R}$

$$F(\theta,R_T,A_T)=F(\theta,\bar{R},\bar{A})+(R_T-\bar{R})\frac{\partial F}{\partial\bar{R}}(\theta,\bar{R},\bar{A})+\tfrac{1}{2}(R_T-\bar{R})^2\frac{\partial^2F}{\partial\bar{R}^2}(\theta,\bar{R},\bar{A})+\Delta F_T\ , \tag{B1a}$$

where

$$\Delta F_T=(A_T-\bar{A})\frac{\partial F}{\partial \bar{A}}(\theta,\bar{R},\bar{A}) +(A_T-\bar{A})(R_T-\bar{R})\frac{\partial^2 F}{\partial \bar{R}\partial \bar{A}}(\theta,\bar{R},\bar{A}) . \tag{B1b}$$

There are no second derivatives with respect to $\bar{A}$ because F is linear in A_τ [see Eq. (3.4a)].

For SCX we need to calculate the correction

$$\Delta F^{(0+)}=\frac{1}{\sqrt{T}}\frac{1}{2T+1}\frac{1}{T+1} \times\{(2T^2-1)(\Delta F_T-\Delta F_{T-1}) +T(2\Delta F_{T+1}-\Delta F_T-\Delta F_{T-1})\} \tag{B2a}$$

[see Eq. (14a) of I]. The single difference in Eq. (B2a) is, from Eq. (B1),

$$\Delta F_T-\Delta F_{T-1}=(A_T-A_{T-1})\frac{\partial F}{\partial \bar{A}}+\tfrac{1}{2}(R_T-R_{T-1})(A_T+A_{T-1}-2\bar{A})\frac{\partial^2 F}{\partial \bar{R}\partial \bar{A}} , \tag{B2b}$$

where we have used the definition of $\bar{R}$, Eq. (3.17b) [also see Eq. (27d) of I]. Now consider the double difference in Eq. (B2a),

$$2\Delta F_{T+1}-\Delta F_T-\Delta F_{T-1}=(2A_{T-1}-A_T-A_{T-1})\frac{\partial F}{\partial \bar{a}}+[(A_{T+1}-\bar{A})(2R_{T+1}-R_T-R_{T-1}) -\tfrac{1}{2}(A_T-A_{T-1})(R_T-R_{T-1})]\frac{\partial^2 F}{\partial \bar{R}\partial \bar{A}} . \tag{B3}$$

The expression is simplified if we choose $\bar{A}=A_{T+1}$ and we find

$$\Delta F^{(0+)}=\frac{1}{\sqrt{T}}\frac{1}{2T+1}\frac{1}{T+1}\left[\Delta S^{(0+)}\frac{\partial F}{\partial \bar{A}}+\Delta P^{(0+)}\frac{\partial^2 F}{\partial \bar{R}\partial \bar{A}}\right] , \tag{B4a}$$

where

$$\Delta S^{(0+)}=[(2T^2-1)(A_T-A_{T-1})+T(2A_{T+1}-A_T-A_{T-1})] , \tag{B4b}$$

$$\Delta P^{(0+)}=\tfrac{1}{2}(R_T-R_{T-1})[(2T^2-1)(A_T+A_{T-1}-2A_{T+1})-T(A_T-A_{T-1})] . \tag{B4c}$$

For DCX we need the correction

$$\Delta F^{(-+)}=\left[\frac{2T-1}{T}\right]^{1/2}\frac{1}{T+1}\frac{1}{2T+1}[(T+1)(\Delta F_T-\Delta F_{T-1})-T(\Delta F_{T+1}-\Delta F_T)] . \tag{B5}$$

The quantity $\Delta F_T-\Delta F_{T-1}$ was evaluated in Eq. (B2), but now we need it for

$$\bar{R}=\tfrac{1}{2}(R_{T+1}+R_{T-1}) ,$$

Eq. (3.18b) [see also Eq. (28d) of I]. We find

$$\Delta F_T-\Delta F_{T-1}=(A_T-A_{T-1})\frac{\partial F}{\partial \bar{A}}-\tfrac{1}{2}(A_{T-1}-A_T)(R_{T-1}-R_{T+1})\frac{\partial^2 F}{\partial \bar{R}\partial \bar{A}} , \tag{B6}$$

where we have defined $\bar{A}=A_T$. Next we evaluate

$$\Delta F_{T+1}-\Delta F_T=(A_{T+1}-A_T)\frac{\partial F}{\partial \bar{A}}+\tfrac{1}{2}(R_{T+1}-R_{T-1})(A_{T+1}-A_T)\frac{\partial^2 F}{\partial \bar{R}\partial \bar{A}} , \tag{B7}$$

where we have used

$$\bar{R}=\tfrac{1}{2}(R_{T+1}+R_{T-1})$$

and $\bar{A}=A_T$. Therefore,

$$\Delta F^{(-+)}=-\left[\frac{2T-1}{T}\right]^{1/2}\frac{1}{T+1}\frac{1}{2T+1}\left\{\Delta S^{(-+)}\frac{\partial F}{\partial \bar{A}}+\Delta P^{(-+)}\frac{\partial^2 F}{2\bar{R}\partial\bar{A}}\right\}, \tag{B8a}$$

$$\Delta S^{(-+)}=(T+1)(A_T-A_{T-1})-T(A_{T+1}-A_T)\,, \tag{B8b}$$

$$\Delta P^{(-+)}=\tfrac{1}{2}(R_{T+1}-R_{T-1})[(T+1)(A_{T-1}-A_T)-T(A_{T+1}-A_T)]\,. \tag{B8c}$$

The derivatives in these formulas are obtained from Eq. (3.4a)

$$\frac{\partial F}{\partial\bar{A}}=\bar{R}J_0(q\bar{R})\,, \tag{B9a}$$

$$\frac{\partial^2 F}{\partial\bar{R}\partial\bar{A}}=J_0(q\bar{R})-q\bar{R}J_1(q\bar{R})\,. \tag{B9b}$$

The main results of this appendix are Eqs. (B4), (B8), and (B9).

APPENDIX C: EXPLICIT EXPRESSION FOR ΔR_{ij} AND ΔA_{ij}

Our goal is now to express ΔR_{ij} and ΔA_{ij} in the form given in Eqs. (3.13a) and (3.14a). Consider first ΔR_{ij}. In I it was shown how to solve Eq. (3.4e) for the differences of radii appearing in Eqs. (3.5), (3.6), (3.9), and (3.10). These differences were expressed in terms of three quantities $\Delta R_{ij}(1)$, $\Delta R_{ij}(2)$, and $\Delta R_{ij}(3)$. The quantity $\Delta R_{ij}(3)$ is zero in the present work, because we assume that the neutrons and protons have the same diffuseness. It is more convenient to combine $\Delta R_{ij}(1)$ and $\Delta R_{ij}(2)$, and the result is

$$R_i-R_j\equiv\Delta R_{ij}=2a_{ij}\left[\frac{\mathrm{Im}\tilde{\chi}_i(\bar{R})-\mathrm{Im}\tilde{\chi}_j(\bar{R})}{\mathrm{Im}\tilde{\chi}_i(\bar{R})+\mathrm{Im}\tilde{\chi}_j(\bar{R})}\right], \tag{C1a}$$

where the quantity a_{ij} is

$$a_{ij}=\tfrac{1}{2}(a_i+a_j)\,, \tag{C1b}$$

with a_i and a_j given by Eq. (3.4d). There are six complex numbers, $\Lambda_0^{(1)}$, $\Lambda_1^{(1)}$, $\tilde{\Lambda}_0^{(2)}$, $\tilde{\Lambda}_1^{(2)}$, $\tilde{\Lambda}_2^{(2)}$, and $\tilde{\Lambda}_3^{(2)}$, specifying $\tilde{\chi}_\tau(b)$ in Eq. (3.1). The quantity ΔR_{ij} depends only on the imaginary parts of these quantities, and in what follows we simplify the equations by taking $\Lambda_j^{(i)}$ to mean $\mathrm{Im}\Lambda_j^{(i)}$ unless specified otherwise. The terms $\Lambda_0^{(1)}\rho$ and $\tilde{\Lambda}_0^{(2)}\rho^2/\rho_0$ naturally belong together, as do

$$\Lambda_1^{(1)}\Delta\rho\gamma^{(1)}(i)$$

and

$$\tilde{\Lambda}_1^{(2)}\frac{\rho\Delta\rho}{\rho_0}\gamma^{(1)}(i)\,,$$

so we define two auxiliary quantities,

$$W_0=\Lambda_0^{(1)}+\tilde{\Lambda}_0^{(2)}\rho/\rho_0\,, \tag{C2a}$$

$$W_1=\Lambda_1^{(1)}+\tilde{\Lambda}_1^{(2)}\rho/\rho_0\,. \tag{C2b}$$

We will expand Eq. (C1) and keep all corrections to the C and D coefficients in Eqs. (3.11) and (3.12) linear in $\tilde{\Lambda}^{(2)}$, W_0, and W_1. The final expressions will be expressed in terms of ratios of the $\tilde{\Lambda}_j^{(i)}$ and W. For example, substitution of Eq. (3.2) into Eq. (C1a) and expanding to the required order in density yields

$$\Delta R_{ij}=a_{ij}\frac{\Delta\rho}{\rho}\left\{\frac{W_1}{W_0}\Gamma_{ij}^{(1)}+\frac{\tilde{\Lambda}_2^{(2)}}{W_0}\frac{\Delta\rho}{\rho_0}\Gamma_{ij}^{(2)}+\frac{\tilde{\Lambda}_4^{(2)}}{W_0}\frac{\Delta\rho}{\rho_0}\Gamma_{ij}^{(4)}+\frac{\Delta\rho}{\rho}\left[\frac{\tilde{\Lambda}_5^{(2)}}{W_0}\frac{\rho}{\rho_0}-\frac{1}{2}\left[\frac{W_1}{W_0}\right]^2\right]\Gamma_{ij}^{(3)}\right\}. \tag{C3}$$

The quantity a_{ij} is worked out in Appendix D and yields

$$a_{ij}\simeq a_\rho\frac{\Lambda_0^{(1)}}{W_0}-\frac{a_\rho}{2}\frac{\Delta\rho}{\rho}[\gamma^{(1)}(i)+\gamma^{(1)}(j)]\phi\frac{\rho}{\rho_0}\,, \tag{C4}$$

and combining this with Eq. (C3)

$$\Delta R_{ij}=a_\rho\frac{\Delta\rho}{\rho}\left\{\Gamma_{ij}^{(1)}\left[\frac{W_1}{W_0}\frac{\Lambda_0^{(1)}}{W_0}\right]+\frac{\Lambda_0^{(1)}}{W_0}\frac{\tilde{\Lambda}_2^{(2)}}{W_0}\frac{\Delta\rho}{\rho_0}\Gamma_{ij}^{(2)}+\frac{\Lambda_0^{(1)}}{W_0}\frac{\tilde{\Lambda}_4^{(2)}}{W_0}\frac{\Delta\rho}{\rho_0}\Gamma_{ij}^{(4)}+\frac{\Gamma_{ij}^{(3)}}{2}\frac{\Delta\rho}{\rho}\left[-\left[\frac{W_1}{W_0}\right]^2\frac{\Lambda_0^{(1)}}{W_0}-\phi\frac{W_1}{W_0}\frac{\rho}{\rho_0}+2\frac{\Lambda_0^{(1)}}{W_0}\frac{\tilde{\Lambda}_5^{(2)}}{W_0}\frac{\rho}{\rho_0}\right]\right\}. \tag{C5}$$

The quantity ϕ is defined in Eq. (D9b). The C coefficients, defined in Eq. (3.13a), may now be read off from Eq. (C5); they are listed in Eq. (3.13).

We next evaluate ΔA_{ij} to obtain the D coefficients. The quantity A_i is defined in Eq. (3.4b) in terms of Y_i, given in Eq. (3.4c). Because Y_i involves the real part of U, we will characterize Y_i in terms of the two quantities y_0 and y_1, defined as

$$y_0 \equiv \frac{\mathrm{Re}\Lambda_0^{(1)} + \mathrm{Re}\tilde{\Lambda}_0^{(2)}\rho/\rho_0}{W_0} , \tag{C6}$$

$$y_1 \equiv \frac{\mathrm{Re}\Lambda_1^{(1)} + \mathrm{Re}\tilde{\Lambda}_1^{(2)}\rho/\rho_0}{W_0} . \tag{C7}$$

In terms of y_0 and y_1 we write Y_i as

$$Y_i \simeq y_0 + \left[y_1 - y_0 \frac{W_1}{W_0} \right] \frac{\Delta\rho}{\rho} \gamma^{(1)}(i) + \left[\frac{\mathrm{Re}\tilde{\Lambda}_2^{(2)} - y_0 \tilde{\Lambda}_2^{(2)}}{W_0} \right] \frac{\Delta\rho^2}{\rho\rho_0} \gamma^{(2)}(i)$$
$$+ \left[\frac{\mathrm{Re}\tilde{\Lambda}_4^{(2)} - y_0 \tilde{\Lambda}_4^{(2)}}{W_0} \right] \frac{\Delta\rho^2}{\rho\rho_0} \gamma^{(4)}(i) + \left[\frac{\rho}{\rho_0} \left[\frac{\mathrm{Re}\tilde{\Lambda}_5^{(2)} - y_0 \tilde{\Lambda}_5^{(2)}}{W_0} \right] - \left[y_1 - y_0 \frac{W_1}{W_0} \right] \frac{W_1}{W_0} \right] \left[\frac{\Delta\rho}{\rho} \right]^2 \gamma^{(1)2}(i) , \tag{C8}$$

where we have retained only lowest-order terms in the y and $\tilde{\Lambda}_2$ parameters. An expression for A_i follows from straightforward algebra, which we omit. The result is, to lowest order in y_i and $\tilde{\Lambda}^{(2)}$,

$$A_i = k a_i \{ \tan^{-1} y_0 + i[C + \ln\ln 2 + \tfrac{1}{2}\ln(1+y_0^2)] \}$$
$$+ k a_\rho \left\{ \left[y_1 - y_0 \frac{W_1}{W_0} \right] \frac{\gamma^{(1)}(i)}{1+y_0^2} \frac{\Delta\rho}{\rho} + \frac{(\Delta\rho)^2}{\rho\rho_0} \left[\frac{\mathrm{Re}\tilde{\Lambda}_2^{(2)} - y_0 \tilde{\Lambda}_2^{(2)}}{W_0(1+y_0^2)} \right] \gamma^{(2)}(i) + \frac{(\Delta\rho)^2}{\rho\rho_0} \left[\frac{\mathrm{Re}\tilde{\Lambda}_4^{(2)} - y_0 \tilde{\Lambda}_4^{(2)}}{W_0(1+y_0^2)} \right] \gamma^{(4)}(i) \right.$$
$$\left. + \left[\frac{\Delta\rho}{\rho} \right]^2 \left[\frac{\rho}{\rho_0} \left[\frac{\mathrm{Re}\tilde{\Lambda}_5^{(2)} - y_0 \tilde{\Lambda}_5^{(2)}}{W_0} \right] - \left[y_1 - y_0 \frac{W_1}{W_0} \right] \frac{W_1}{W_0} \right] \frac{\gamma^{(1)2}(i)}{1+y_0^2} \right\} . \tag{C9}$$

In order to find A_i to lowest order in y_i and $\Lambda^{(2)}$, we keep a_i to lowest order in $\Lambda^{(2)}$. We see from Eqs. (D7) and (D9)

$$a_i \simeq a_\rho \frac{\Lambda_0^{(1)}}{W_0} , \tag{C10}$$

so, from Eqs. (C9), (C10), and the definitions in Eq. (3.14a), we read off the D coefficients. They are listed in Eq. (3.14).

APPENDIX D: EXPRESSIONS FOR a_i AND a_{ij}

Recall that $a_i(R)$ is defined by

$$a_i(R) = -\frac{\mathrm{Im}\tilde{\chi}_i(R)}{\mathrm{Im}\tilde{\chi}_i'(R)} . \tag{D1}$$

Defining $u_i^{(1)}$ and $u_i^{(2)}$ as the imaginary parts of the linear and quadratic terms in $\tilde{\chi}_\tau$ in Eq. (3.3a), Eq. (D1) may be written

$$a_i(R) = -\frac{u_i^{(1)} + u_i^{(2)}}{u_i^{(1)'} + u_i^{(2)'}} . \tag{D2}$$

Dividing numerator and denominator by $u_i^{(1)}$, we find

$$a_i = a_\rho \left[\frac{1 + u_i^{(2)}/u_i^{(1)}}{1 + 2u_i^{(2)}/u_i^{(1)}} \right] , \tag{D3}$$

where we assume that $u^{(2)}$ falls off exactly twice as fast as $u^{(1)}$,

$$u^{(2)'}/u^{(1)} = 2u^{(2)}/u^{(1)} , \tag{D4}$$

which is only approximately true for realistic choices of densities. Equation (D3) may now be written

$$a_i = a_\rho \left[\frac{V_0(i)+V_1(i)}{V_0(i)+2V_1(i)+V_2(i)} \right] , \tag{D5}$$

where

$$V_0 = W_0\rho + W_1\gamma^{(1)}(i)\Delta\rho , \tag{D6a}$$

$$V_1 = \Lambda_2^{(2)}\frac{\Delta\rho^2}{\rho_0}\gamma^{(2)}(i) + \Lambda_4^{(2)}\frac{\Delta\rho^{(2)}}{\rho_0}\gamma^{(4)}(i) + \tilde{\Lambda}_5^{(2)}\frac{\Delta\rho^2}{\rho_0}\gamma^{(1)^2}(i) , \tag{D6b}$$

$$V_2 = \Lambda_0^{(2)}\frac{\rho^2}{\rho_0} + \tilde{\Lambda}_1^{(2)}\frac{\rho\Delta\rho}{\rho_0}\gamma^{(1)}(i) . \tag{D6c}$$

Dividing numerator and denominator in Eq. (D5) by $V_0(i)$ we find

$$a_i = a_\rho \left[\frac{1+V_1(i)/V_0(i)}{1+2V_1(i)/V_0(i)+V_2(i)V_0(i)} \right] = a_\rho - a_\rho \left[\frac{V_1(i)+V_2(i)}{V_0(i)} \right] . \tag{D7}$$

Thus,

$$a_i + a_j = 2a_\rho - a_\rho \left[\frac{V_1(i)+V_2(i)}{V_0(i)} + \frac{V_1(j)+V_2(j)}{V_0(j)} \right] . \tag{D8}$$

In order to evaluate Eq. (D7) we need an expression for

$$\frac{V_1(i)+V_2(i)}{V_0(i)} .$$

From Eq. (D6) we have

$$\frac{V_1(i)+V_2(i)}{V_0(i)} = \frac{\Lambda_0^{(2)}}{W_0}\frac{\rho}{\rho_0} + \gamma^{(1)}(i)\frac{\Delta\rho}{\rho_0}\phi , \tag{D9a}$$

where

$$\phi = \frac{\Lambda_1^{(2)}}{W_0} - \frac{\Lambda_0^{(2)}}{W_0}\frac{W_1}{W_0} . \tag{D9b}$$

The quantity $a_i + a_j$ is needed only to first order in density since ΔR_{ij} in Eq. (C3) contains an overall factor of $\Delta\rho/\rho$. Thus we write

$$a_{ij} \equiv \frac{a_i+a_j}{2} = a_\rho - a_\rho \left[\frac{\Lambda_0^{(2)}}{W_0}\frac{\rho}{\rho_0} + \tfrac{1}{2}(\gamma^{(1)}(i)+\gamma^{(1)}(j))\frac{\Delta\rho}{\rho_0}\phi \right] . \tag{D10}$$

*Permanent address: Nuclear Physics Laboratory, University of Colorado, Boulder, CO 80309.

[1]For a complete set of references to previous work, see J. Alster and J. Warszawski, Phys. Rep. 52, 87 (1979); G. R. Burleson, in Proceedings of the LAMPF Workshop on Nuclear Structure with Intermediate-Energy Probes, Los Alamos National Laboratory Report LA-8303-C, 1980, p. 195.

[2]M. B. Johnson, Phys. Rev. C 22, 192 (1980), referred to as I.

[3]H. Baer, J. D. Bowman, M. D. Cooper, F. H. Cverna, C. M. Hoffman, M. B. Johnson, N. S. P. King, J. Piffaretti, E. R. Siciliano, J. Alster, A. Doren, S. Gilad, M. Moinester, P. R. Bevington, and E. Winkelmann, Phys. Rev. Lett. 45, 982 (1980).

[4]C. L. Morris, H. A. Thiessen, W. J. Braithwaite, W. B. Cottingame, S. J. Greene, D. B. Holtkamp, I. B. Moore, C. F. Moore, G. R. Burleson, G. S. Blanpied, G. H. Daw, and A. J. Viescas, Phys. Rev. Lett. 45, 1233 (1980).

[5]M. B. Johnson and E. R. Siciliano, Phys. Rev. C (to be published).

[6]L. S. Kisslinger, Phys. Rev. 98, 761 (1955).

[7]R. Mach, Nucl. Phys. A205, 56 (1973).

[8]M. Thies, Phys. Lett. 63B, 43 (1976).

[9]G. E. Brown, B. K. Jennings, and V. Rostokin, Phys. Rep. 50, 227 (1979).

[10]N. J. DiGiacomo, A. S. Rosenthal, E. Rost, and D. A. Sparrow, Phys. Lett. B66, 421 (1977).

[11]K. Stricker, H. McManus, and J. A. Carr, Phys. Rev. C 19, 929 (1979); K. Stricker, J. A. Carr, and H. McManus, *ibid.* 22, 2043 (1980).

[12]K. Stricker, Michigan State University thesis, 1979 (unpublished).

[13]R. Amado, F. Lenz, and K. Yazaki, Phys. Rev. C 18, 918 (1978).

[14]R. S. Bhalerao, L. C. Liu, and C. M. Shakin, Phys. Rev. C 21, 2103 (1980).

[15]W. B. Cottingame and D. B. Holtkamp, Phys. Rev. Lett. 45, 1828 (1980).

[16]M. B. Johnson, in Proceedings of the LAMPF Workshop on Nuclear Structure with Intermediate Energy Probes, Los Alamos Scientific Laboratory Report LA-8303-C, 1980, p. 130.

[17]M. Koren, Ph.D. thesis, MIT, 1969 (unpublished).

[18]G. A. Miller and J. E. Spencer, Ann. Phys. (N.Y.) 100, 562 (1976).

[19]G. A. Miller and J. E. Spencer, Phys. Lett. 53B, 329 (1974).

[20]N. Auerbach and N. Van Giai, Phys. Rev. C 24, 782

(1981).

[21]R. A. Eisenstein and G. A. Miller, Comput. Phys. Commun. 8, 130 (1974).

[22]M. B. Johnson and H. A. Bethe, Commun. Nucl. Part. Phys. 8, 75 (1978).

[23]J.-F. Germond and M. B. Johnson, Phys. Rev. C 22, 1622 (1980).

[24]S. J. Wallace, Ann. Phys. (N.Y.) 78, 190 (1973).

[25]M. B. Johnson and H. A. Bethe, Nucl. Phys. A305, 418 (1978); M. B. Johnson and B. D. Keister, *ibid.* A305, 461 (1978).

[26]The spreading of the Δ_{33} resonance is clearly seen in the phenomenological analysis of elastic scattering; for example, see Y. Horikawa, M. Thies, and F. Lenz, Nucl. Phys. A345, 386 (1980).

[27]M. B. Johnson, in *Proceedings of the International School of Physics, "Enrico Fermi" Course LXXIX,* edited by A. Molinari (North-Holland, Amsterdam, 1981), p. 412.

[28]This cancellation is not manifest in the theory, but the physics of the definition of $\lambda_4^{(2)}$ requires that the cancellation occur.

[29]J. W. Negele and D. Vautherin, Phys. Rev. C 5, 1472 (1972).

[30]K. K. Seth, invited paper presented at the Intermediate-Energy Nuclear Chemistry Workshop, Los Alamos National Laboratory, Los Alamos, New Mexico, 1980 (unpublished).

[31]R. L. Burman, M. P. Baker, M. D. Cooper, R. H. Heffner, D. M. Lee, R. P. Redwine, J. E. Spencer, T. Marks, D. J. Malbrough, R. M. Preedom, R. L. Holt, and B. Zeidman, Phys. Rev. C 17, 1774 (1978).

[32]K. K. Seth, S. Iverson, H. Nann, M. Kaletka, J. Hird, and H. A. Thiessen, Phys. Rev. Lett. 43, 1574 (1979).

[33]S. J. Greene, W. J. Braithwaite, D. B. Holtkamp, W. B. Cottingame, C. F. Moore, C. L. Morris, H. A. Thiessen, G. R. Burleson, and G. S. Blanpied, Phys. Rev. Lett. 88B, 62 (1979).

[34]S. J. Green *et al.*, Phys. Rev. C 25, 927 (1982); S. J. Greene, M. B. Johnson, and E. R. Siciliano (unpublished).

[35]L. C. Liu, Los Alamos Report LA-UR-81-3592, 1981.

[36]D. A. Sparrow and A. S. Rosenthal, Phys. Rev. C 18, 1753 (1978).

[37]M. Kaletka and K. K. Seth, private communication.

[38]H. T. Fortune, S. J. Green, C. F. Moore, and C. L. Morris, Phys. Rev. C 25, 2142 (1982).